國立臺灣大學電機資訊學院生醫電子與資訊研究所

碩士論文

Graduate Institute of Biomedical Electronics and Bioinformatics
College of Electrical Engineering and Computer Science
National Taiwan University

Master Thesis

馬兜鈴酸腎毒性在嚙齒類動物的代謝體學研究

Metabolomics Study of Aristolochic Acid Nephrotoxicity in Rodents

蔡東銘

Dong-Ming Tsai

指導教授：曾宇鳳 博士

郭錦樺 博士

Advisor: Yufeng J. Tseng, Ph.D.

Ching-Hua Kuo, Ph. D.

中華民國 98 年 7 月

July, 2009

致謝

最要感謝的是我的指導老師曾宇鳳博士和郭錦樺博士，曾老師在資訊學上的學養引領我進入跨領域的生物醫學研究。郭老師對整個實驗設計及儀器分析的指導讓我一步步的學習以致論文的完成。

整個動物實驗的部份是在毒理學研究所康照洲老師的實驗室完成的。特別感謝陳小白助理完成實驗並提供實驗結果讓我能研究分析。實驗樣品的核磁共振譜是送到中央研究院完成的，期間全賴藥學研究所的伊琳學姐處理與保存樣品。

感謝三源學長以他資訊領域的專長幫我更正了許多錯誤。每當我面對複雜難解的資料分析時，實驗室的同學們總是不吝於幫忙，在此致上無限的感謝。

最後謝謝我的家人(阿心、昀叡和筑宇)，他們的支持和鼓勵是我最大的動力。

摘要

馬兜鈴酸具腎毒性，過去傳統中藥裏常使用的馬兜鈴酸屬的植物含有此物質。本實驗研究馬兜鈴酸標準品、馬兜鈴草果實及含馬兜鈴草的中藥複方補肺阿膠湯 3 種物質在嚙齒類動物上的腎毒性，並以代謝體學方法分析尿液核磁共振氫譜在馬兜鈴酸腎病變中的變化。實驗目的在初步探討如何以容易取得之尿液來建立腎毒性之診斷模式。實驗共分 4 部份進行，一為大鼠以胃灌食馬兜鈴酸標準品測試。二為小鼠以胃灌食馬兜鈴酸標準品測試。三為小鼠以胃灌食馬兜鈴草果粉末測試。四為小鼠以胃灌食補肺阿膠湯粉末測試。實驗收集每日尿液樣本並冷凍保存以備分析，實驗結束後犧牲鼠隻取其肝腎做病理分析。

結果：大鼠馬兜鈴酸標準品給藥 5 劑後腎病理檢查顯示高劑量組有 1-3 度的急性腎小管間質病變。小鼠馬兜鈴酸標準品給藥 10 劑後，高低劑量組皆有 3-4 度的急性腎小管間質病變。小鼠馬兜鈴草給藥 21 劑後，低及中劑量組有 1-2 度而高劑量組有 3-4 度之急性腎小管間質病變。小鼠補肺阿膠湯給藥 20 劑後，低劑量組有 2 度而高劑量組有 3-4 度之急性腎小管間質病變。尿液核磁共振氫譜以主成份分析法分析各實驗中各個組別在同一天之分數圖，結果發現大鼠馬兜鈴酸標準品給藥後 2 天 3 組皆能分群。小鼠馬兜鈴酸標準品給藥後 8 天高劑量組能與其他 2 組分群，10 天時給藥的 2 組能與對照組分群。小鼠馬兜鈴草給藥後 8 天高劑量組能與其他 3 組分群，10 天時高劑量與中劑量組能與對照及低劑量組分群。小鼠補肺阿膠湯各組則至給藥後 16 天仍未見分群。以 t 檢定比對給藥組與對照組尿液中內生

代謝物隨時間相對濃度變化發現大鼠馬兜鈴酸標準品實驗早期時甘氨酸、琥珀酸、氧化三甲胺及 2-酮戊二酸有下降的現象，而到晚期時糖類、尿囊素、肌酐、二甲基甘胺酸、2-酮戊二酸及氧化三甲胺有上升現象($p < 0.05$)。小鼠馬兜鈴酸酸標準品實驗之代謝物濃度有明顯變化者相對較少，但在實驗後期可見給藥組有丙氨酸、乳酸及甲酸平均濃度相對增加之現象。

結論：馬兜鈴酸標準品及含有此物質的中草藥馬兜鈴和其複方補肺阿膠湯在鼠類是有腎毒性的。以主成份分析尿液的核磁共振氫譜可以分辨出有發生腎病變的組別，其代謝體的濃度變化也可進一步分析找出相關的生物標誌。但在含低劑量馬兜鈴酸的複方補肺阿膠湯在本實驗中則未能以主成份分析法從尿液分析出小鼠發生的腎病變，這有待進一步的代謝體學分析研究。

關鍵詞：

馬兜鈴酸、馬兜鈴、補肺阿膠湯、主成份分析、代謝體學、核磁共振氫譜

Abstract

Aristolochic acid (AA) is a potent nephrotoxic agent that can be found in several herbs of the genus *Aristolochia.* It was once commonly used in traditional Chinese medicine remedy. In this study, we applied our metabolomics platform of the ^{1}H NMR spectroscopy on urine with principal component analysis (PCA) to detect and further dissect the nephrotoxicity in rodent of four AA containing materials, AA standard, Madouling, an AA containing herb *Aristolochia contorta* and Bu-Fei-A-Jiau-Tang (BFAJT), a herb compound containing *Aristolochia contorta*. The aim was to use the easy available urine samples to establish a model for early diagnosis of nephrotoxicity. The experiment was divided into four parts. The first was rat AA experiment. The second was mouse AA experiment. The third was mouse Madouling experiment. The fourth was mouse BFAJT experiment. Urine samples were collected daily and freeze-dried for storage. All animals were euthanized after experiment and their kidneys and livers procured for pathological studies.

Results: In the rat AA experiment, pathology showed grade (gr.) 1-3 acute renal tubulointerstitial necrotic change (ATIN) after 5 doses in the high dose group. In the mouse AA experiment, 10 doses were given. Both high and low dose group showed gr. 3-4 ATIN. In the mouse Madouling experiment, 21 doses were given. It was gr. 1-2 for low and moderate groups, and gr. 3-4 ATIN for the high dose group. In the BFAJT

experiment, 20 doses were given. It was gr. 2 ATIN in the low dose group and gr. 3-4 in the high dose group. PCA scoring plots for the urine NMR spectral chemical shifts variables showed early cluster at 2 day and later for each group in the rat AA experiment. In the mouse AA experiment, the high dose group was clustered from the other 2 groups at day 8. It was at day 10 that the 2 dose groups were clustered from the control group. In the mouse Madouling experiment, the high dose group clustered from all other 3 groups. It was at day 10 that the high dose and the moderate dose groups clustered together from the other 2 groups. In the BFAJT experiment, PCA scoring plots failed to classify across control and dose groups even at day 16.

The endogenous metabolites assigned from NMR spectroscopy and their integral concentration among dose and control groups were tested by t-test. In the rat AA experiment glycine, succinate, 2-oxoglutarate and trimethylamine-N-oxide (TMAO) were decreased in the dose groups in earlier days of the experiment. At later days, sugar, allantoin, creatine, dimethylglycine, 2-oxoglutarate and TMAO were increased in the dose groups ($p < 0.05$). In the mouse AA experiment no significant metabolite difference was noted, only alanine, lactate and formate had more than two fold change at day 10.

In conclusion, AA standard, Madouling and BFAJT were all nephrotoxic. PCA scoring plots for the urine NMR spectroscopy collected from living animals showed the

ability to classify the dose and control groups days before confirming the renal pathology. But toxicity classifying failed in the mouse BFAJT experiment by PCA scoring plot. Further metabolomics study is expected to resolve this issue.

Keywords:

Aristolochic Acid, Aristolochia contorta, Madouling, Bu-Fei-A-Jiau-Tang, 1H NMR Spectroscopy, Metabolomics, Principal Component Analysis, Nephrotoxicity

Contents

List of Figures

List of Tables

Chapter 1. Background and Literature Review

1.1 Introduction

The plant of genus *Aristolochia* was widely used for herbal medicine in the ancient time, but its toxicity in humans was only noticed a little more than a decade ago [3, 4].

Traditional Chinese medicine (TCM) as alternative remedies is prevalent worldwide [5]. Herbal medicine may be connected to toxicity and its pathophysiology may be not well delineated because of their complex in nature of their biochemical components. Usually, toxicity of herbal medicine can only be evaluated from experience or out-dated literatures, therefore the safety measures in Chinese herbs are usually overlooked [6-8].

Metabolomics, a newly developed "omics" technology, can be applied in studying xenobiotic toxicity. The difficulties in analyzing herbal medicine are their complex ingredient and many unknown interactions with living system. Metabolomics, the holistic and systematic study of metabolites in an organism, can be applied to resolve such issue especially in Chinese herb toxicity. In this research we established a metabolomics study model to study the nephrotoxicity of herbs of *Aristolochia* species.

1.2 Literature Review

1.2.1 Aristolochic acid nephropathy

1.2.1.1 *Aristolochia* herbs

In 1993, an unusually form of severe renal failure occurred in several women in a Belgium clinic. All patients who developed renal dysfunction took pills to reduce weight. The slimming pills were composed of several drugs in addition to some Chinese herbs. A herb called "Fangchi" was noted to be misused as "Fangji" which is the plant *Stephania tetrandra*. The misused drug "Fangchi" is *Radix Aristolochia fangchi* and it was later proved to be the cause of the severe nephropathy found [9, 10]. More than one hundred women who took the herb developed renal dysfunction and many of them progressed to end-stage renal disease. During follow-ups a large portion of these patients developed urothelial malignancy even stop taking the pills [4, 11]. The renal disease was initially termed as "Chinese herb nephropathy" for its correlation with herbal medicine. It was found that aristolochic acids in the plant *A. fanchi* was the major cause of nephropathy [12]. Aristolochic acid, a major ingredient in these herbs was proved to be the causal agent for this form of nephropathy. The rapidly progressive fibrosing nephropathy is then called "aristolochic acid nephropathy" to be precise [3].

In the past, herbs of genus *Aristolochia* were commonly used in TCM. They were used for therapy in a wide spectrum of morbidity such as snake bites, rheumatism, gout and festering wounds [13]. Usually herbs of *Aristolochia* species were given in the form of Chinese herbal compound remedies. For instance, Bu-Fei-A-Jiau-Tang

(BFAJT), a decoction used in the treatment of air way troublesome. It contains Madouling (*Fructus Aristolochia*), the fruit of *Aristolochia contorta* [14]. Long-Dan-Xie-Gan-Tang, also a herbal compounds, contains *A. manshuriensis*. The compound was used in various systemic symptoms in terms of TCM, such as liver and bile insufficiency [15, 16].

Before AA containing products were prohibited because of its toxicity in humans, the uses of *Aristolochia* herb were common based on their wide therapeutic spectrum. Following the episode happened in Belgium, advanced Aristolochic acid nephropathy had been reported in many countries including Taiwan [17, 18].

1.2.1.2 Toxicology Related to Aristolochic Acids

Aristolochic acids, which are derivatives of nitrophenanthrene, are characteristic chemical constituents of *Aristolochia* species [19]. Among these structurally related chemicals, AA-I, the 8-methoxy-3,4-methylenedioxy derivative, and AA-II, the 3,4-methylenedioxy derivative, are the major components of the AA containing *Aristolochia* species (Figure 1) [20].

After ingestion into the body, AA-I and AA-II are metabolized and may form DNA adducts. Several studies revealed that DNA adducts can induce genotoxicity and they are found mostly in renal tissue in rats [21]. In human exposed to aristolochic acids, AA DNA adducts can be found in kidney and urothelial tissue. The AA DNA adducts

are proved to be involved with genotoxicity and carcinogenicity [13, 20].

With different duration and doses of exposure to AA, the nephropathy may be acute, subacute or chronic. Mengs reported the lethal dose 50 (LD_{50}) of a single oral AA was 138.9-203.4 mg/kg for rat and 55.9-106.1 mg/kg for mouse [22]. In female Wistar rat given a single oral doses of AA 10 mg/kg, mild acute renal damage was observed by a rise in the mitotic index of renal tubular tissue after three days. Severe renal tubular necrosis was observed at a dose of 100 mg/kg [23]. At lower dose but longer exposure to AA, acute renal damage can be found within weeks in rodents. The dose needed to induce renal damage is lower for mouse than for rat. For example, in BALB/c mouse received oral AA salt 2.5 mg/kg/day for 10 doses within 2 weeks, severe degeneration of renal tubular epithelium was found [24]. As for Wistar rat, if AA was given subcutaneously in 10 mg/kg/day for five weeks, there was necrosis of renal tubules with interstitial lymphocyte infiltration at day 10. Renal tubular fibrosis could be detected at day 35. The chronic renal pathological change is similar to abnormalities found in human [10]. The carcinogenic effect of AA occurs at lower AA dosed with longer exposure. With oral administration of AA at the dose of 0.1 mg/kg/day in rats, malignant tumors developed after 12 to 16 months. For high dose at 10 mg/kg/day, malignancy occurred within 6 months [25].

It was noted that AA induced defective activation of anti-oxidative enzymes and

mitochondial damage in rat. The oxidative stress resulted in repaired regeneration, proximal tubular cells and eventually lead renal tubular atrophy [26]. The expression of several oxidative stress related factors such as vascular endothelial growth factor, hypoxia inducible factor I alpha was increased in cells within damage tubulointerstitial area [27].

1.2.1.3 Evaluation of Aristolochic Acid Nephropathy

Serum urea and creatinine are commonly used for kidney injury detection and monitoring. In acute renal injury both serum markers can only be detected to a significant detectable elevation after loss of more than 60% renal function. Besides, several non-renal factors can influence the serum level of these markers. Serum urea level fluctuates with hydration state, amount of nitrogen containing diet intake, liver disease status, using of corticosteroid and gastrointestinal bleeding related azotemia. Under the influence of these non-renal factors, it is unreliable for renal injury detection. Serum creatinine is one of the traditional indicators for significant renal injuries and is useful for evaluation of renal function change during progression of chronic renal failure. However it is not sensitive and not injury site specific [28]. In an acute kidney injury, only more than 50% increase of serum creatinine level is defined as significant change. There are also several non-renal factors to influence the serum creatinine level. Mass bulk, sex, age and muscular morbidity can much influence the

serum creatinine level [29]. Hauet *et al.* used ischemic reperfusion model to test the correlation of creatinine clearance with renal injury, and found that creatinine clearance did not decrease until one week after ischemia. Before the decrement of creatinine clearance was detected, several metabolites such as citrate, trimethylamine oxide (TMAO), dimethylamine, lactate and acetate were found significantly increased in urine [30]. Urine biomarkers such as human kidney injury molecule-1 (KIM-1) and *N*-acetyl-β-D-glucosaminidase (NAG) are site specific and present only in renal injury state. To increase the sensitivity and specificity by using urine enzyme to detect renal injury and the injured site, Han, et. al. recommended a combination of several renal injury related urine enzymes such as matrix metalloproteinase-9, NAG and KIM-1 as biomarkers [31]. Undoubtedly, the approach for acute renal injury diagnosis requests expensive test kits and sophisticated sample preparatory procedures .

Moreover, combinatorial screen of them is difficult and not widely accepted. Other non-invasive diagnostic methods use renal imaging instruments (ultrasonography and nuclear scintigraphy) to detect renal injury. These imaging studies are used as secondary diagnosis to differentiate possible associated morphological changes or vascular anomaly, and have limited values as a primary tool to diagnose acute renal injury [30, 32]. Renal biopsy for histopathological study remains the landmark for renal injury diagnosis. The invasiveness and little versatility prohibited this method

to be used in early detection of renal injuries when repeated measurements are required. Despite low sensitivity, examination of serum creatinine and urea are still widely applied for renal injuries detection. Due to their low sensitivity and site specificity, development of improved new diagnostic method is important.

There are many metabolites in urine and their concentrations may change due to renal injury. With the screening of all urinary metabolite, it may provide valuable information on AA nephropathy.

1.2.2 Metabolomics

1.2.2.1 Definition and Technologies used

To determine whether a new xenobiotic compound is nephrotoxic, we may extrapolate results from animal experiments to human. To confirm the existence of xenobiotic nephrotoxicity, histopathological examination is a gold standard. But to detect xenobiotic nephrotoxicity in early stage, non-invasive detection methods in animal experiment are favored.

After the human genome decoded in 2000s, the study of disease from molecular genetic level was made possible. The term genomics is then used to describe the study of whole genome. Since a genome contains sequence of billions of nucleotides, traditional genetic analyzing method cannot efficiently delineate changes from the complicated genetic networks. Microarray as a powerful tool has made tenable the

study of genomics and transcriptomics. Bioinformatics is rapidly developed to encounter the analysis of huge amount of data produced from microarray experiments [33]. Although microarray studies the functional gene expression, in aspect to effects on the cellular response it's still in the upstream stage. Proteomics studies enzymatic, signaling and immunological changes after gene expression. Through protein control and their enzymatic function metabolic pathways work to maintain a living system. Proteomics can hardly predict what really happened in a living system and changes of metabolism with time [34]. Metabolite changes, both temporal and as a whole, are the phenotype through changes of genes, proteins and environmental stimulation. Through analysis of metabolite changes in perturbed metabolic pathways, the effect of interaction of genes and environment can be estimated. The idea of a comprehensive study of metabolites is what metabolomics originated.

As early 1940s the concept to study pathophysiological changes in an organism by metabolic profiles from tissue or biofluids had been mentioned [35]. But their methods for metabolic profiling were primitive and intangible for duplication. In 1970s, a hyphenated technology that combined gas chromatography, mass spectroscopy (MS) and chemometric analysis was applied to metabolic profiling for differentiating normal from pathological state and for drug metabolism [35]. In 1980s, it was reported that proton nuclear magnetic resonance (^{1}H NMR) spectroscopy of rat urine

can be a novo tool to detect nephrotoxicity induced by mercuric chloride. In 1999, the term "metabonomics" was used to describe a series of works utilizing ^{1}H NMR spectroscopy for metabolic profiling study [36]. Metabonomics is defined as "the quantitative measurement of the dynamic multiparametric metabolic response of living systems to pathophysiological stimuli" [36]. The term "metabolomics" was first mentioned in 2002 to link between genotype and phenotype [37]. Genomics, transcriptomics, proteomics and metabolomics are a cascade in systems biology and metabolomics is the end of this cascade to delineate what is the result of biological perturbation (Figure 2).

1.2.2.1.1 NMR Spectroscopy

NMR spectroscopy and MS are the two most commonly used analytical instruments for metabolomics. We used NMR spectroscopy for our study, and the principle of NMR spectroscopy is hereby introduced in brief.

A hydrogen nucleus which contains one unpaired proton that spins. The spin possesses an angular momentum P, and it is associated with a moment μ, i.e. $\mu=\gamma P$ (μ: magnetic moment, γ: gyromagnetic ratio, 2.68 X 108 for ^{1}H, P: angular momentum) (figure 4a).

The interaction of external magnetic field interacts with the spins of protons to produce Larmor precession. The frequency is proportional to the external magnetic

field. i.e. $\omega_L=\gamma B_0$ (ω_L :frequency, B_0: external static magnetic field) (figure 4b).

With the influence of external magnetic field, the energy state of protons can be separated into two status, it's called Zemann effect. The distribution of protons in these two status is determined by Boltzmann distribution. An energy difference is between the status. i.e. $\Delta E=(\gamma h/2\pi)B_0$ (ΔE: energy difference between the two quantum status, h: Planc constant) (Figure 4c). Larmor precession frequency can be calculated as: $\nu_0=(\gamma/2\pi)B_0$.

Finally a net internal magnetic field M_0 is produced under external magnetic field. With radiofrequency (RF) to change the direction of M_0 and by the detection of ν_0 during relaxation, we can detect a signal and its called free induction decay (FID) (figure 4d).

When RF pulses are produced perpendicularly to B_0, M_0 will turn toward a direction perpendicular to both RF wave and B_0, we may assign it as M. If RF pulses are stopped, M will relax back to M_0, and two vectors can be analyzed: M_Z and M_{xy} (figure 4e).

The relaxation parameters can be used in NMR technology, to suppress water signal during sample solution signal acquisition. A selective frequency is given during relaxation delay to produce the effect [38].

The spin of a proton may be changed slightly due to nearby electronic clouds in a

molecule. The change is the chemical shift, a small value as compared to a reference frequency unaffected by electronic clouds effect. The chemical shift value is represented in part per million (ppm) and it is calculated as $(\nu_A-\nu_S/\Omega)\times10^6$, ν_A is the detected proton frequency and ν_S is the frequency of a standard reference chemical such as tetramethylsilane. With the chemical shift, ^{1}H NMR spectroscopy analyzes proton containing molecule and differentiate different proton groups in the molecule.

MS is used widely in metabolomics as well. MS is more sensitive to differentiate than NMR spectroscopy. A separation technique is necessary before MS, these may include liquid chromatography, gas chromatography or capillary electrophoresis. Comparing with NMR spectroscopy, sample preparation is simple for NMR. NMR is robust for sample analysis and better in quantification while MS needs standards for scaling [39].

1.2.2.2 Metabolomics in Toxicological Studies

Metabolomics has been used in the study of aristolochic acid nephrotoxicity [1, 40-44]. NMR spectroscopy can be used in AA nephrotoxicity study. Zhang, et al. studied AA nephrotoxicity. AA standard 10 mg/kg/day was given to Wistar rats by peritoneal injection for 5 days. Serum samples were analyzed by NMR spectroscopy with principal component analysis (PCA). Scoring plot from PCA showed similar clustering between AA dosed group and another nephrotoxic agent $NaCrO_4$ [45]. In

the same and expanded set of experiment, PCA scoring plots of NMR spectra of urine samples showed time-dependent analogous clustering with different nephrotoxic agents [1]. Zhao et al. used *Aristolochia manshuriensis* decoction to study its toxicity in rats. The AA containing herb was given through oral route in divided doses comparable to AA 7-10.4 mg/kg/day. Metabolomic analysis of NMR spectra from urine samples showed dose and time dependent results. Histopathological examination of rat renal tissue showed acute renal tubulointerstitial changes at day 6 post dosing [46, 47]. From analysis of NMR chemical shift variables, several fluctuated metabolites between control and dosed groups were deduced. Other metabolomics studies AA nephrotoxicity used LC-MS as the analysis tool in rats, both AA standard and *Aristolochia manshuriensis* were tested [40, 41, 44]. The metabonomics studies showed possibility of early detection of AA nephrotoxicity. The easiness of its collection and richness in metabolic information made urine samples an ideal material to study AA nephrotoxicity.

Different *Aristolochia* species may have different metabolic pattern in vivo than AA standard due to their inherent complexity in composition [48]. In TCM, multiple different herbs are usually mixed together as a remedy formula. As previous metabolomics studies focused on rat and tested the acute toxicity of AA standard and *A. manshurienesis* using high dose. To further delineate AA nephrotoxicity, we tried

other *Aristolochia* species and herbal compounds containing *Aristolochia* plants. Furthermore, AA nephrotoxicity may differ in different species [49], as we know, metabolomics studies on AA nephrotoxicity were done on rat and not on mouse yet. Since mouse is a common experimental animal, metabolomics of AA nephrotoxicity in mouse may help find more metabolite changes.

Urine is commonly used in metabolomics study of nephrotoxicity. Urine contains metabolites through the kidney and their concentrations may fluctuate with time, genetic and environmental changes. Urine is also easy to be collected and metabolomic analysis on nephrotoxicants may be recognized with specific pattern.

1.2.3 Chemometrics and Pattern Recognition Technology

The International Chemometrics Society (ICS) defines chemometrics as "the science of relating measurements made on a chemical system or process to the state of the system via application of mathematical or statistical methods". With computer technology, the complex ^{1}H NMR spectra with numerous peaks of different size and their respective chemical shifts can be compared and analyzed.

1.2.3.1 Data Processing of NMR Spectroscopy

The ^{1}H NMR spectrum contains information of all chemical shifts from metabolites in the biofluids sample tested. The chemical shifts of a metabolite may not be identical across samples due to pH, temperature changes, solvent strength, magnetic

field inhomogeneity and metabolite concentration. To quantifying different metabolite concentration across samples, alignment of relevant peaks is necessary before multivariate analysis. Metabolite concentrations fluctuate in a large range in urine due to concentrating effect of renal tubules, normalization of concentrations across sample is required as well. A commonly used method for normalization is "integral normalization" which integrate all peaks in a spectrum and all peaks are divided by the sum value. In urine samples with high metabolites concentration fluctuation, this method provides a linear balance of metabolite concentration between samples. But in case of toxicological study, a few of the urine metabolites may change in large magnitude that metabolites of low concentration will be further diminished in their concentration with this method. Other methods of normalization have been proposed. Probabilistic quotient normalization (PQN) utilized statistic method to find a median factor between the reference and target spectra after integral normalization. It was robust to avoid suppression of low concentration metabolites by removing the involvement of non-linear large metabolite concentration [50]. Log transformation of peak concentration is also utilized in integral normalization for detection of low concentration metabolites [51]. As PQN minimized the effects of very high metabolites concentration, we didn't apply log transformation for our spectral peak intensities. Dynamic time warping, correlation optimized warping (COW) and

Bayesian approach [52] were used for alignment and normalization [53]. In a doxorubicin toxicological study in rats using 1H NMR spectroscopy, COW has been used for alignment of NMR spectra [54]. In our study we applied baseline correction, integral normalization, PQN and spectra binning prior to multivariate analysis.

1.2.3.2 Unsupervised Pattern Recognition

Principal component analysis (PCA) is used in unsupervised pattern analysis of NMR spectra. Multivariate complexity of chemical shifts and their peak height formed ^{1}H NMR spectra can be diminished to several principal components that encoded original data information. With the first two or three orthogonal principal components that can explain most part of variance difference in rotated axes with least covariance, different patterns of metabolic profiles can be classified in a scoring plot. The major responsible variable of chemical shifts that may represent certain metabolites can be analyzed through loadings plot. Coefficients for variables in loadings signify their importance in principal components and the spectral area of major loadings may contain metabolites which differentiate the phenotypes. Here we introduce our PCA method.

1.2.3.2.1 Principal Component Analysis

Principle component analysis (PCA) is a statistical technique that changes multidimensional variables into orthogonal components. A ^{1}H NMR data matrix is

composed of samples with their respective signal intensities in a range of chemical shifts. A variable-variable covariance matrix from the data matrix can be decomposed to orthogonal eigenvectors and their respective eigenvalues. Projection of the data matrix to the eigenvectors minimizes the covariance and a few of these orthogonal components with the largest eigenvalues can be selected to represent sample scores. Through PCA, NMR spectra which form the multidimensional data matrix can be represented by a few principal components to diminish dimensions.

1.2.3.3 Metabolites Assignment for NMR Spectroscopy

Metabolomics analyzed toxicological effects from metabolite changes through pattern recognition. The metabolites that fluctuate during intoxication are traced through 1D ^{1}H NMR spectroscopy. Several metabolites are abundant in urine and exist prominent peaks. The proton containing molecules have specific chemical shifts patterns and can be identified through targeted profiling. Targeted metabolic profiles from known metabolite peaks can help identify metabolites from their peaks pattern. Creatinine in ^{1}H NMR has two single peaks at 3.04 and 4.06 ppm. 2-Oxoglutarate can be identified by two triplet around 2.42 and 2.99 ppm. Statistical total correlation spectroscopy (STOCSY) is a statistical method to analyze correlation of different peaks across 1D NMR spectra from experimental samples [55]. The different peaks of the same molecule fluctuate synchronized with its respective concentrations in different

samples and from these correlated peaks the metabolite can be identified. Moreover, peaks of different metabolites along a metabolic pathway may show significant correlation either positive or negative and it may help find perturbed metabolic pathway.

Different species of animals may respond differently to xenobiotic toxicity. Rats and mice are commonly used experimental animals in toxicological studies. Mice are small and easier to handle than rats and have more different transgenic subspecies to choose. In an experiment on 2-bromoethanamine hydrobromide (BEA) nephrotoxicity study, mice are less sensitive to BEA. Taurine was not increased in the rat urine and might indicate less nephrotoxic tendency in mouse because the osmoprotective effects of taurine [56]. In our study, we used both rats and mice for AA nephrotoxicity experiments, the response may differs among difference species.

1.3 Aim

Aristolochic acid is a potent nephrotoxic agent, and widely used in Traditional Chinese Medicine. Although association between aristolochic acid or aristolochic acid containing herb and nephrotoxicity has been established, detailed biomarkers and related pathway was not identified. The consequence between compound remedy containing Aristolochiaceae herb and nephrotoxicity was unknown. With the metabolomics technology in the study of aristolochic acid related nephropathy may provide new ways in diagnosis and treatment of toxic nephropathy.

We designed and established a nephrotoxic study model based on metabolomics to help early detection and understanding of aristolochic acid nephropathy with AA standard, herb and compound remedy.

Chapter 2. Materials and Methods

2.1 Aristolochic Acid Sources

Authentic standard aristolochic acid, Madouling (*Fructus Aristolochia contorta*) and a compound remedy Bu-Fei-A-Jiau-Tang (BFAJT) were used.

Aristolochic acid was purchased from Acros Organics (New Jersey, USA). The content of AA-I was 96% and AA-II 4%.

Madouling powder was purchased from Sheng Chang Pharmaceutical Co., Ltd (Taipei, Taiwan). The dried decoction powder was filtered and extracted from boiled herb. The dosing sample was a mixture of the decoction and corn oil. The content of AA-I is 24.17 mg/gm and AA-II 2.04 mg/gm for the dosing sample.

BFAJT powder was purchased from Sheng Chang Pharmaceutical Co., Ltd (Taipei, Taiwan). The dried decoction powder was filtered and extracted from boiled herb. The dosing sample was a mixture of the decoction and corn oil. The content of AA-I is 3.749 mg/g and AA-II 0.169 mg/g for the dosing sample. The BFAJT powder is composed of donkey hide gelatin 45 g, Madouling 15 g, apricot seed 6 g, great burdock fruit 7.5 g, rice 30 g and honey fried licorice root 7.5 g (http://www.sacredlotus.com/formulas/get.cfm/chinese_formula/bu_fei_e_Jiao_tang/).

2.2 In vivo Experiments and Sample Preparation

Wistar rats and BALB/c mice (all from National Taiwan University Laboratory

Animal Center, Taipei, Taiwan) were used in different study sets.

2.2.1 Rat

The rat experiment was designed for studying AA standard toxicity. Nine female rats weighing 250-300 g were divided into 3 groups and each contained 3 rats. Rat was placed in metabolic cages in an air conditioned room with free water and food intake. On day 0, all urine and blood samples were collected after 16 hours of fasting. While the control group received the dosing vehicle, the dosing groups were given AA standard orally, with 4 mg/day for the low dose group and 8 mg/day for the high dose group. AA was dissolved in polyethylene glycol 400 (PEG 400) solution and was given for 5 consecutive days. The control group was given PEG solution of the same concentration only. AA dosing was initiated after urine and blood collection on day 0. Day 1 was defined as 24 hours after the initiation of AA dosing. It was counted on the same time interval for later experimental days. AA and vehicle were given through oral gavage. Urine samples were collected twice daily from one day prior to AA dosing. The collected urine was centrifuged at 3000 rpm for 15 min immediately, and the clear suspension was stored at -80°C after adding 150 mM sodium azide with a ratio of 280 μl to 20 μl. Blood samples are collected daily from the day AA is given. Ether anesthesia was given before blood sampling from the rat tail. The blood samples were centrifuged and serum urea, creatinine, aspartate transferase and alanine

transferase were checked by a biochemical analyzer (Fujifilm Dri-Chem 3500s). Body weight change was recorded daily.

After experiment, all rats were euthanized and liver and kidney were procured for pathological study. The degree of renal lesions was graded from one to four depending on severity: 1 = minimal (< 1%); 2: slight (1-25%); 3 = moderate (26-50%); 4 =moderate/severe (51-75%); 5 = severe/high (76-100%) [57]. It was according to the renal histopathological findings of anatomical site of lesions (cortex to medulla), location of renal tubular lesion (proximal to distal, focal to locally extensive), morphology of renal tubular lesion (dilatation with or without hyaline cast to necrosis) and patterns of inflammation (acute to subacute).

2.2.2 Mouse

There were three experiments using mouse. In the first set of mouse experiment, 10 mice weighing 15-20 g were divided into 3 groups. They were control (n=3), low AA group dosed with 5 mg/kg/day (n=3) and high AA group dosed with 7.5 mg/kg/day (n=4). AA was dissolved in corn oil with a concentration of 1 and 1.5 mg/ml. The vehicle and AA were given 5 days per week. Urine samples were collected once daily, and processed as last rat experiment. Under ether anesthesia, blood samples were collected by orbital bleeding 3 times per week. Blood was sent for biochemical studies after centrifugation and all mice were euthanized after experiment for pathological

analysis.

In the second set of mouse experiment, , the toxicity of Madouling herb was studied. Twelve mice were divided into 4 groups, they were control, low dose, moderate dose and high dose groups. Each group contains 3 mice and the dose of Madouling was 559, 1118 and 2236 mg/kg for low, medium and high dose groups. The three doses of Madouling were equivalent to 0.69, 1.38 and 2.75 mg of AA-I. The Madouling powder of 559, 1118 and 2234 mg were each dissolved in 10 ml secondary deionized water and given to mice through gavage. Collection and handling of urine and blood samples were similar as described in the first mouse experiment. At the end of experiment, histopathological study of kidneys and liver for all mice were performed after euthanasia.

In the third set of mouse experiment, the toxicity of BFAJT was studied. Nine mice were divided into 3 groups, they were control, low dose and high dose groups. Each group contains 3 mice and the dose of Bu-Fei-A-Jiau-Tang (BF) was 2 g and 4 g/kg for low and high dose groups. The doses of BFAJT were equivalent to 0.25 mg and 0.5 mg of AA-I. Collection and handling of urine and blood samples were similar as described in the first mouse experiment. At the end of experiment, histopathological study of kidneys and liver for all mice were performed after euthanasia.

All 4 experiments are summarize in Table 1.

2.3 NMR Measurement and Pattern Recognition Investigation

2.3.1 NMR Spectra Acquisition

^{1}H NMR spectroscopy was performed from collected urine samples from rats and mice. The freeze-dried rat urine was thawed and 200 μl of phosphate buffer (pH 7.4) was added into 400 μl urine sample to minimize variations in the pH of the urine sample. For mouse urine, 200 μl of phosphate buffer (pH 7.4) was added into a mixture of 200 μl mouse urine sample with 200 μl deionized H_2O. Six hundred μl of supernate obtained by centrifugation was pipetted into 5 mm NMR tubes with 50 μl D_2O containing 5 mM trimethylsilyl-3-propionic acid-d4 2,2,3,3-sodium salt (TMSP) for an internal reference standard (δ 0.00) and field frequency locking. 1H NMR spectra were recorded on 600 MHz NMR system (Bruker Biospin, Rheinstetten, Germany) with an acquisition time of 2.73 s at 298 K. Water signals were suppressed by presaturation pulse sequence noesypr1d (RD-90°-t_1-90°-t_m-90°-AQ, radiofrequency presaturation at the water resonance (δ=4.701 ppm) during RD (1s) and t_m (100 ms)). The sum of 128 transients was recorded with 16 k data points and eight dummy scans. All spectra were referenced to TMSP at δ0.00 ppm.

2.3.2 Spectral Data Processing

Each ^{1}H NMR free induction decay (FID) data was transformed to 1D spectrum in

ACD/Labs v10.0 1D NMR manager (Advanced Chemistry Development, Inc, Canada). The spectral data was exported to a 16 k data points text file recording chemical shifts and their respective signal intensities. The spectral raw data was then sent to R statistical software for baseline correction and binning. The spectral intensities were binned in 0.04 ppm from 0 ppm to 10 ppm using programs written with R statistical software. The standard intensity was scaled to 100 with a multiplying factor calculated and all the rest integrated intensities of the same spectrum was scaled by multiplying the scaling factor of the standard. Intensity data of water (4.5-5.5 ppm) and urea (5.5-6.0 ppm) were set to zero. To normalize metabolite concentration among these spectra, a probabilistic quotient normalization algorithm was performed. A detailed data processing procedures are described in Appendix.

2.3.3 Statistical Methods

Univariate data was analyzed with Student t test with R software, $p < 0.05$ was considered as significant.

2.3.3.1 PCA

The binned and normalized spectral data was analyzed by principal component analysis after centering and standardization. Scoring plots with two dimensional principal component were drawn for spectral classification. Loadings plots were drawn to search for significant chemical shift variables.

2.4 Metabolite Assignment

Urine metabolites were assigned by referencing peak pattern and chemical shifting to NMR library in human metabolic database (HMDB) [58], and reports on rodent urine ^{1}H NMR [59, 60].

Chapter 3. Results

3.1 In vivo Experiment

3.1.1 Rat on AA

3.1.1.1 Clinical Signs and Biochemical Parameters

The mean body weight (BW) measured in the AA standard experiment showed significant BW loss from day 2 to 5 in the high dosed group as compared with the mean BW of the same group at day 1 (Figure 4). The mean daily urine volume of day 2 to day 4 was not significantly different from day 2, although it showed an increasing tendency in the high dose group (Figure 5). Mean serum urea of the high dosed group was increased significantly at day 2 and day 4 than that of the same group at day 1 (Figure 6). Serum creatinine also showed a range of 0.1-0.2 mg/dl in all rats and there was no significant change found.

3.1.1.2 Pathology

No significant histopathological change of kidney were found in control and low dose group. One rat of high dose group showed grade 1 renal injury and another 2 rats grade 3. The pattern of renal injury was prominent for proximal renal tubule and glomerular morphology was intact (Figure 7). All liver specimen showed no significant finding.

3.1.1.3 Metabolomic Profiling

54 NMR spectra of urine samples were analyzed. A series of spectra of one rat in high dose AA group is shown in Figure 10. Assigned metabolites in aliphatic and aromatic region are annotated. Day 0 urine showed low peak intensities in the chemical shifts region 3.5-4.0 ppm which was compatible with their fasting status.

PCA scoring plots showed time-dependent clustering among 3 groups. On day 0, sample points in the PC1 and PC2 coordinate were clustering together. All groups were unclassified until day 2 after 48 hours initiating AA dosing (Figure 8).

Loading plot for PC1 and PC2 showed several significant variables. The significant binned segments were inspected to see if the spectral contained peaks that can be assigned to endogenous metabolites. After normalization to the creatinine peak at 3.06 ppm, the relative ratio to creatinine of each identified metabolites were compared among different groups and days (Figure 9). On day 4 or day 5, the concentration of several metabolites were different between the control and dosed rats. Dimethylglycine, 2-oxoglutarate, taurine, glycine, sugar, creatine, allantoin and hippurate were significantly increased or decreased as compared to control group.

3.1.2 Mouse on AA

In the first mouse experiment tested with AA, urine samples collected at day 0, 1, 3, 8 and 10 of all ten mice were sent for ^{1}H NMR spectroscopy. Collection of two urine samples were failed, one at day 0 was of the low dose group due to poor urine quality

and another at day 10 was of the high dose group due to mortality on day 9. Thus, it resulted 48 NMR spectra for analysis. The experiment stopped on day 12 after 9 doses were given.

3.1.2.1 Clinical Signs and Biochemical Parameters

The mean body weight (BW) measured in the mouse AA standard experiment showed significant mean BW loss of the low dose group at day 11 than the mean BW of the same group at day 0 (Figure 12). Mean serum urea (UN) of was significant higher at day 4 and 11 for high dose group and at day 4 as compared to the same group at day 2 (Figure 13). Serum creatine was within the range of 0.1 to 0.4 mg/dl and showed a tendency of increment in the high dose group (Figure 14).

3.1.2.2 Pathology

No significant histopathological change of kidney were found in the control group. Both low and high dose groups showed grade 3-4 tubulointerstitial acute renal injury with preserved glomerular morphology (Figure 15). All liver specimen showed no significant finding.

3.1.2.3 Metabolomic Profiling

48 NMR spectra of urine samples were analyzed. A series of urine spectra collected at day 0, 1, 3, 8 and 10 of one mouse from the high dose AA group is shown in Figure 16. Assigned metabolites in aliphatic and aromatic region are annotated.

PCA scoring plots showed time-dependent clustering among 3 groups. On day 0 and day 2, there was no clustering across three groups. At day 3, the high dose group became clustering and was separated form the other two groups till day 10. The trajectory of a high dose mouse which died on day 9 was labeled as "H1". A mouse of the low dose group which failed to have day 0 urine collected was labeled as "L2" Figure 17).

Loading plot for PC1 and PC2 showed several significant variables (Figure 18). The significant binned segments were inspected to see if the spectral contained peaks that can be assigned to endogenous metabolites. After normalization to the creatinine peak at 3.06 ppm, the relative ratio to creatinine of each identified metabolites were compared among different groups and days (Figure 19). On day 4 or day 5, the concentration of several metabolites were different between the control and dosed rats. Lactate, succinate, glycine and TMAO were significantly increased or decreased as compared to the control group.

3.1.3 Mouse on Madouling

In the second mouse experiment tested with Madouling, urine samples of all 12 mice on day 0, 1, 3, 8 and 10 were collected. One mouse of the high dosed group died on day 9. Thus 59 urine samples were sent for ^{1}H NMR spectroscopy. An NMR spectrum of a mouse of the moderate dose group was distorted too much to be analyzed.

Therefore 58 NMR spectra were amenable for analysis. The experiment stopped on day 21 after 21 doses were given.

3.1.3.1 Clinical Signs and Biochemical Parameters

The mean body weight (BW) measured in the mouse Madouling experiment showed significant mean BW loss of the moderate and high dose group from day 1 to day 20 (Figure 20). Mean serum urea (UN) was not increased until day 20 in the high dose group, statistically not estimatable due to only 2 mice left (Figure 21). Serum creatine was within the range of 0.2 to 1.1 mg/dl and showed no significant changes among all groups (Figure 22).

3.1.3.2 Pathology

No significant histopathological change of kidney were found in the control group. Both low and moderate dose groups showed grade 1-2 tubulointerstitial renal injury. The high dosed group showed grade 3-4 tubulointerstitial renal injury with preserved glomerular morphology (Figure 23). All liver specimen showed no significant finding.

3.1.3.3 Metabolomic Profiling

58 NMR spectra of urine samples were analyzed. A series of urine spectra collected at day 0, 1, 3, 8 and 10 of one mouse from the high dose Madouling group is shown in Figure 24. Assigned metabolites in aliphatic and aromatic region are annotated.

PCA scoring plots showed the clustering of high dose group was classified from other 3 groups at day 8. Two survived mice of the high dose group at day 10 were separated from other groups too. The scoring points labeled "M1", "M2" and "M3" showed distribution of respective mouse in the moderate dose group at day 8 and 10 (Figure 25).

Loading plot for PC1 and PC2 showed several significant variables (Figure 26). The significant binned segments were inspected to see if the spectral contained peaks that can be assigned to endogenous metabolites. After normalization to the creatinine peak at 3.06 ppm, the relative ratio to creatinine of each identified metabolites were compared among different groups and days (Figure 27). On day 4 or day 5, the concentration of several metabolites were different between the control and dosed rats. Acetate, dimethylamine (DMA), dimethylglycine (DMG) and TMAO were significantly increased or decreased as compared to control group.

3.1.4 Mouse on Bu-Fei-A-Jiau-Tang

In the third mouse experiment tested with BFAJT, urine samples of all 9 mice on day 0, 2, 6, 10, 13 and 16 were collected. One mouse of the high dosed group died on day 15. Thus 53 urine samples were sent for ^{1}H NMR spectroscopy. The experiment stopped on day 20 after 20 doses were given.

3.1.4.1 Clinical Signs and Biochemical Parameters

The mean body weight (BW) measured in the mouse BFAJT experiment showed significant mean BW loss of the low and high dose group at day 20, and day 10 for the high dose group (Figure 28). Mean serum urea (UN) was increased until day 20 both the control and high dose groups (Figure 29). Serum creatine was within the range of 0.2 to 1.0 mg/dl and showed no significant changes among all groups.

3.1.4.2 Pathology

No significant histopathological change of kidney were found in the control group. The low dose group showed grade 2 tubulointerstitial renal injury. The high dosed group showed grade 2-3 tubulointerstitial renal injury with preserved glomerular morphology (Figure 30). All liver specimen showed no significant finding.

3.1.4.3 Metabolomic Profiling

53 NMR spectra of urine samples were analyzed. A series of urine spectra collected at day 0, 2, 6, 10, 13 and 16 of one mouse from the high dose BFAJT group is shown in Figure 31.

PCA scoring plots showed no group clustering at all time points (Figure 32).

The significant binned segments were inspected to see if the spectral contained peaks that can be assigned to endogenous metabolites. After normalization to the creatinine peak at 3.06 ppm, the relative ratio to creatinine of each identified metabolites were compared among different groups and days (Figure 27). On day 4 or

day 5, the concentration of several metabolites were different between the control and dosed rats. Acetate, dimethylamine (DMA), dimethylglycine (DMG) and TMAO were significantly increased or decreased as compared to control group.

Chapter 4. Discussion

Aristolochic acid is a potent nephrotoxicant. In our experiment, we tested its nephrotoxicity in rat and mouse. To delineate the influence of the nephrotoxicity of AA in its natural biological form, we used AA standard, an AA containing herb Madouling and a herbal compound containing Madouling. The pathological data from our experiment confirmed the nephrotoxicity of AA containing toxicants. We performed four sets of experiments. In the rat AA experiment, under 8 mg/day AA for 5 days, the kidney showed a pattern of acute proximal renal tubular necrosis and relatively preserved glomerular morphology. The low dose rat group received 4 mg/day AA had no significant renal lesions than in the control group. As LD_{50} in female rat had been reported to be a single AA dose of 183.9 mg/kg, for a 200 g rat this may equal to 36 mg of AA [22]. Our AA 4 mg/day group had an accumulative dose of 20 mg after 5 days of dosing and we noted no renal tubulointerstitial lesion. It seemed that a bolus oral AA dose of 36 mg was much toxic than 20 mg divided into 5 days in a 200 g rat. Although there was no pathological renal necrotic lesions in the 4 mg low dose group, the mean BW of this group decreased at day 5 and that may indicate anorectic effect of AA. The BW change of the 8 mg high dose group showed significant decrease since day 2 and indicated more anorectic effect at this dosage. We studied urine volume change and there was a tendency of increased urine output in the 8

mg/day group and this may be resulted from the disturbed water reabsorption in the proximal renal tubule. The mean serum urea increased along with the accumulation of AA dosage in the high dose group and this may indicate renal injury resulting disturbed renal urea excretion. At a dose of 8 mg/day AA for 5 days, the high dosed group showed decreased BW, increased urine volume, serum urea and with a pathological pattern of acute proximal renal tubular injury. At a half dose of 4 mg/day, we did not find significant renal injury.

In the mouse AA experiment, the mean BW of high (7.5 mg/kg/day) and low (5 mg/kg/day) groups was decreased at day 11 as compared with day 0. The mean serum urea increased significantly for the high dose group at day 4 and day 11. The serum creatinine was increased in the high dose group. The two clinical indicators of renal function showed possible renal dysfunction in the high dose group. The pathological finding showed moderate to severe renal interstitial tubular injury in both low and high dose group. Therefore, we detected AA nephrotoxicity in mouse exposed to AA 5 mg/kg/day or high dose after 10 doses given. From the result of our experiment, the mouse was more sensitive to the nephrotoxicity of AA than the rat which did not show pathological renal injury at 4 mg/day (about 20 mg/day) for 5 days. In mouse, the accumulative dose was 50 mg/kg to induce nephrotoxicity and not in rat with 100 mg/kg of AA.

In the mouse Madouling experiment, we used less daily AA dose as considering the volume tolerance of Madouling decoction in mouse through gavage route. We thus increase the experiment duration to 21 days with a gavage feeding volume tolerable for the mouse. The pathological findings of the low dose (559 mg/kg/day) and moderate dose (1118 mg/kg/day) group showed grade 1-2 renal injury and the respective accumulated AA-I dose is 14.5 mg and 29 mg. The renal injuries deteriorated to grade 3-4 for the high dose (2236 mg/kg/day) group which had AA-I accumulated dose of 58 mg. In the low dose group, with daily dose of AA-I 0.69 mg contained in Madouling of 559 mg, we induced renal injury in the low dose and all other higher dose groups after 21 days of dosing. Clinical data of BW and serum urea showed compatible change by AA intoxication.

In the mouse BFAJT experiment, the more feeding bulk volume of this compound further restricted the amount of AA dose. Thus the equivalent AA dose used was even lower than the mouse Madouling experiment. For 4 g BFAJT there contained AA-I 0.5 mg. We gave BFAJT 4 g/kg/day for 20 days in the high dose group. The mean BW was decreased until day 10 for the high dose group and at day 20 for the low dose group (2 g/kg/day). Serum urea did not show tendency of time-dependent increment in dosed groups. A grade 2 renal injury in both dose groups indicated the nephrotoxicity of BFAJT. From these clinical and pathological findings, the nephrotoxicity of AA

showed a tendency of BW decrement and it may be caused by anorectic and diuretic effects of the AA contained.

PCA as a pattern recognition multivariate analysis tool was used for all experiments to classify different dose groups from ^{1}H NMR spectra of urine samples. In the rat AA experiment, clustering of all three groups at day 0 and day one indicated a baseline similarity in their urine metabolites. Day 0 was under fasting status without the interference of diet. Urine of day one was collected after 24 hours of the first AA dose and diet intake. Scoring plot of day one showed neither diet metabolites or AA metabolites in the urine separated samples of different groups. At day 2 to day 5, scoring plots showed separation across control, low dose and high dose groups. Under relatively large dose of AA (we gave 4 and 8 mg/day which is equivalent to 20 and 40 mg/kg/day for a 200 g rat), the clustering of different dose groups as early as day 2 in our scoring plots may indicated change of urine metabolites due to AA nephrotoxicity. Although the low dose group showed no significant renal tubulointerstitial injury at necropsy after 5 doses of 4 mg/day AA, it was possible that the rat urine metabolites changed before the detection of renal morphological change.

We chose a chemical shifts range from 1 to 4.5 ppm rather than using whole spectrum (0 to 10 ppm) in PCA analysis for mouse AA experiment. As signal/noise ratio of the aromatic region of NMR spectrum in the mouse AA experiment was large

by inspection. The scoring plots of the mouse AA experiment showed the urine metabolite change by AA nephrotoxicity was detectable as early as day 3 in both dose groups. The urine sample labeled "L2" of a mouse in the low dose group was unclassified from the control group. As daily urine output in mouse is around 3 ml/day [61], it was possible that contamination from food or other mouse secretion occurred in the urine sample. In the study by Zhang et al. [1], we did not note in their PCA plots a time-dependent clustering of the AA dosed group from the control group. We identified time-dependent PCA clustering of the control group from the dose groups. In a metabolomics study using LC-MS, Chan et al. [44] showed PCA can identify the AA dosed group but there was no pathological information for the experiment.

In the mouse Madouling experiment, PCA scoring plots showed the high dose group clustered from the other groups at day 6 with an accumulative equivalence AA-I of 16.5 mg/kg. At day 10 both high and moderate groups clustered together and were separated from the control and low dose groups. Pathology done after exposure to Madouling dosing for 21 days showed there were renal necrotic injuries for both moderate and high dose groups. PCA analysis at 10 day identified a compatible difference between pathology of groups. With PCA scoring plot, the nephrotoxicity of a daily exposure of Madouling with equivalent dose of 2.75 mg/kg/day in mouse can be detected at day 8 and later.

In the mouse BFAJT experiment, PCA scoring plots failed to classify across different dosed groups. Although pathological finding showed there was renal tubulointerstitial injury in both dose groups after 20 dosed of BFAJT, a PCA scoring plot as late as day 16 did not show clustering of dose groups. The dose of equivalent AA-I was 0.5 mg/kg/day in the high dose group which was not as high as the dose of AA used in previous experiments. The low dose of AA in BFAJT may have more insidious urine metabolite changes detectable. Interaction with other compounds inside BFAJT may also ameliorated the urine metabolite change.

Reviewing previous metabolomics studies on AA nephrotoxicity by urine samples, PCA was applied for group identification. For those experiments using AA standard, the result of PCA scoring plot can successfully classify between control and dosed group. But in the only experiment using *A. manshuriensis* that presented a PCA scoring plot, the group clustering failed (Table 2). We successfully identified between control and dosed groups using PCA for our mouse Madouling experiment and it denoted PCA can identify the status of simple herb nephrotoxicity. For AA containing herbal compound, PCA failed to identify between control and dosed group in this preliminary experiment. More sample size and further metabolomics approach may resolve this difficulty in classifying the dose group.

The loading plots of PCA helped selecting what binned ppm segments contribute

to clustering of dose groups. The NMR signal of proton containing metabolites with chemical shifts within the selected binned ppm segments may be biomarkers for AA nephrotoxicity. As in 1D ^{1}H NMR spectroscopy, it is difficult to identify low concentration metabolites within these selected binned ppm segments. Here we only pointed out the significant binned ppm from the loading plot. However, there were already several urine metabolites identified in ^{1}H NMR spectroscopy either in rat [54, 62] or mouse [59, 63, 64] by their specific peak pattern and chemical shifts. To identify endogenous metabolites with relative high signal intensity, we referred to these papers and assigning identifiable metabolites into our urine spectra. By opening a window with width around 4 ppm, the peak pattern and wave chemical shifts range can be compared across all spectra. After scaling to the creatinine peak intensity of a reference spectrum, the relative concentration of assigned metabolites were compared across all spectra of one of our experiments.

In the rat AA experiment, at day 3, the concentration of glycine, succinate, 2-oxoglutarate and TMAO were decreased in the dose groups than the control group at the same day ($p < 0.05$). At day 5, sugar, allantoin, creatine, dimethylglycine, 2-oxoglutarate and TMAO were significantly increased in the dosed group. At early stage of renal injury, decreased energy metabolism related metabolites such as succinate, and 2-oxoglutarate may indicate mitochondrial injury of renal cells in the dosed group.

Alanine, which is a traditional urine biomarker for renal proximal tubular injury, decreased at 3 day in our study. In a study by Sieber et al., the level of alanine did not change significantly at day 6 under 120 mg/kg/day gentamicin in the rat. Although it increased significantly in earlier days [2]. The structural renal tubule injury may be mild accompanying regeneration mechanism and thus influenced little the proximal renal tubular reabsorption at this stage. Hippurate was increased in the high dose group which was contrary to a study of gentamicin nephrotoxicity in the rat [65]. Dimethylglycine was a renal osmolyte, its increment denoted renal medullary injury. The pattern of urine metabolites change was time and dose dependent. In our study, we have similar metabolite changes as previous reported in a rat AA metabolomics study [1], they were sugar and hippurate (Figure 33).

In the mouse AA experiment, loading plot showed a broad range of significant variables. Although only a few metabolites showed significant concentration change by paired t-test, there were metabolites that showed a tendency of difference among control and dosed groups. The increment of alanine at day 8 and day 10 indicated proximal renal tubular reabsorption perturbed in the dosed mice. Higher urine lactate at day 8 and day 10 in the dose groups showed possible tubular injury.

In the mouse Madouling experiment, the dosed groups showed non-significant increased lactate, glucose and succinate which denoted renal injury. Since PCA

scoring plots showed the high dose group clustered at day 8 and 10, the contribution of unassigned low concentration metabolites difference among control and dose groups should be considered.

As shown in figure 34, urine metabolites did not change significantly in both AA and Madouling experiment in mouse comparing with their control group. With pattern recognition the dosed groups in these two experiments can be identified. A search of lower concentration metabolites may help find more significant biomarkers. In the BFAJT experiment, there were no significantly urine metabolites for the high dose group at day 10 and day 16. Balanced renal injury and tissue recovery may shield the underlying pathological change.

Chapter 5. Conclusion and Future Work

In conclusion, AA standard was nephrotoxic from our pathological results in both rat and mouse. Madouling as an AA containing herb was nephrotoxic for mouse at an AA-I equivalent dose of 0.69 mg/kg/day or more for 21 days. Acute renal injury was induced even at lower dose for BFAJT at 0.25 mg/kg/day (Table 3). PCA scoring plots for urine NMR spectroscopic analysis can classify the existence of nephrotoxicity in three of our four experiments. The failure of our PCA scoring plot to classify the nephrotoxic groups in mouse BFAJT experiment may need more metabonomics technologies to delineate AA toxicity.

We have demonstrated that it is possible to apply metabolomics to early diagnosis of AA nephrotoxicity. As BFAJT nephrotoxicity, there were no endogenous urine metabolites of relatively high concentration significantly different from the control group. More animals for testing and combination with other metabolomics instrument such as LC-MS may help us to further delineate more metabolic perturbation in AA nephropathy.

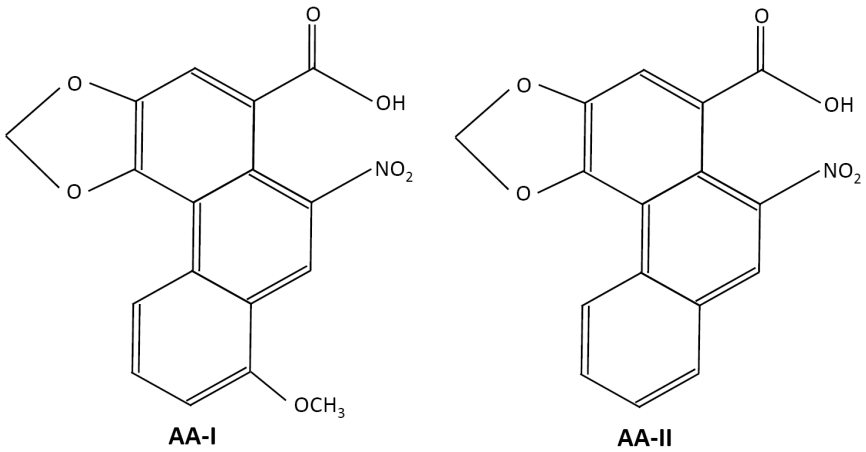

Figure 1. Chemical structure of aristolochic acid I (AA-I) and II (AA-II).

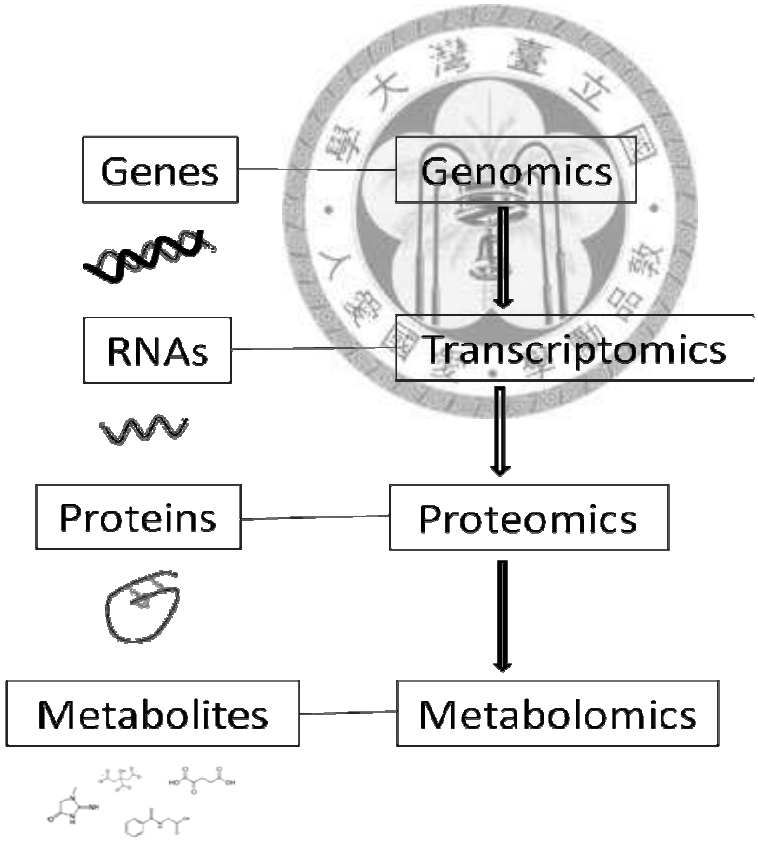

Figure 2. Cascade of "-omics". Metabolomics studies the end point of biological complex system.

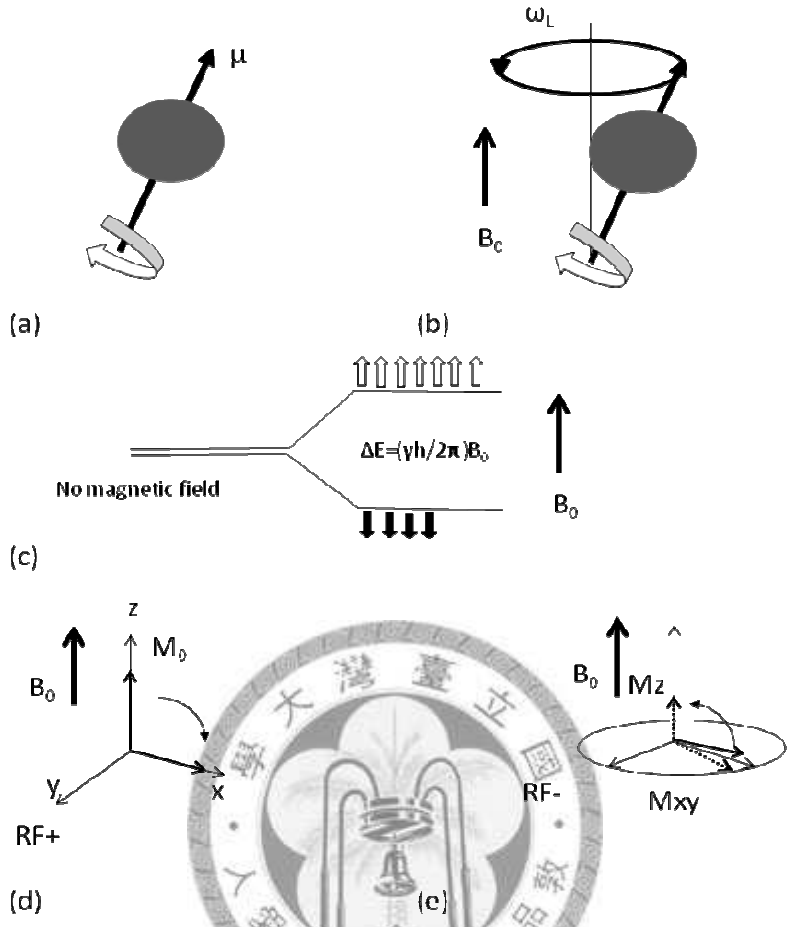

Figure 3. Illustrations of principles of nuclear magnetic resonance. The moment μ comes from the momentum of a proton spin (a). When there is an external magnetic field B_0, a Larmor precession (ω_L) occurs (b). Energy status of protons are divided into two energy level under external magnetic field (c). A radio frequency pulse (RF+) along the y axis will rotate the internal magnetic field produced by Larmor precession M_0, which is directed along the z axis to x axis (d). After the radio frequency pulse ceased (RF-), the rotated magnetic field will relax to two magnetic vectors M_Z and M_{XY} (e).

Table 1. Summary of the four experiments for aristolochic acid nephrotoxicity

Animal and material	Toxicants weight/kg/day	Eq. dose to AA or AA-I (mg)	No. of animals	Solvent	Urine sampling date (No. of NMR spectra)	Notes
Rat AA	Control	0	3	PEG 400	Day 0-5 (n=54)	
	AA 20 mg	20	3			
	AA 40 mg	40	3			
Mouse AA	Control	0	3	Corn oil	Day 0,1,3,8,10 (n=48)	1 urine loss on day 0; 1 mouse died on day 9
	AA 5.0 mg	5	3			
	AA 7.5 mg	7.5	4			
Mouse Madouling	Control	0	3	Double deionized H_2O	Day 0,1,3,8,10 (n=58)	1 NMR not amenable; 1 mouse died on day 9
	M 559 mg	0.69(AA-I)	3			
	M 1118 mg	1.38(AA-I)	3			
	M 2236 mg	2.75(AA-I)	3			
Mouse BFAJT	Control	0	3	Double deionized H_2O	Day 0, 2, 6, 10,13 & 16 (n=53)	1 mouse died on day 15
	BFAJT 2 g	0.25(AA-I)	3			
	BFAJT 4 g	0.5(AA-I)	3			

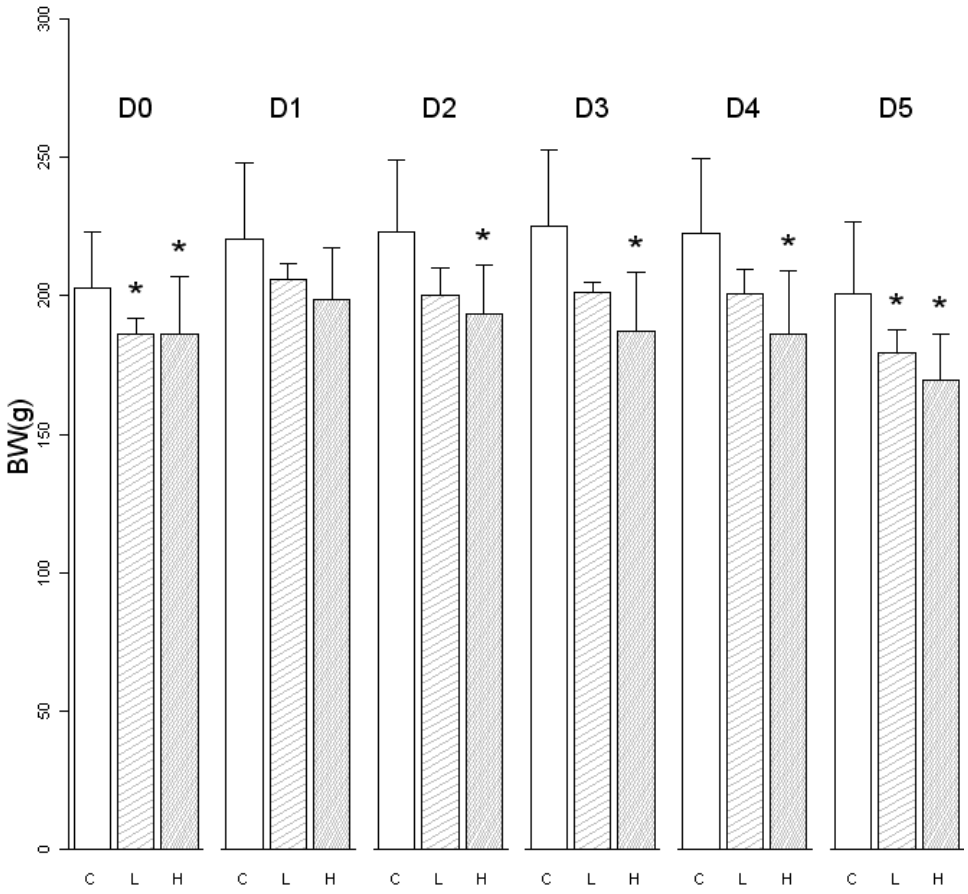

Figure 4. Mean body weight (BW) of three groups of rat in AA experiment. The mean BW of dosed groups was tested with the same group at day 1 (D1). Mean BW of high AA dosed group was significantly different from that at D1 at all other days. It was day 0 (D0) and day 5 for low dose group. * $p < 0.05$, paired t-test. Error bars are the standard deviation of group means. Groups were C: control (n=3), L: low (n=3), H: high (n=3).

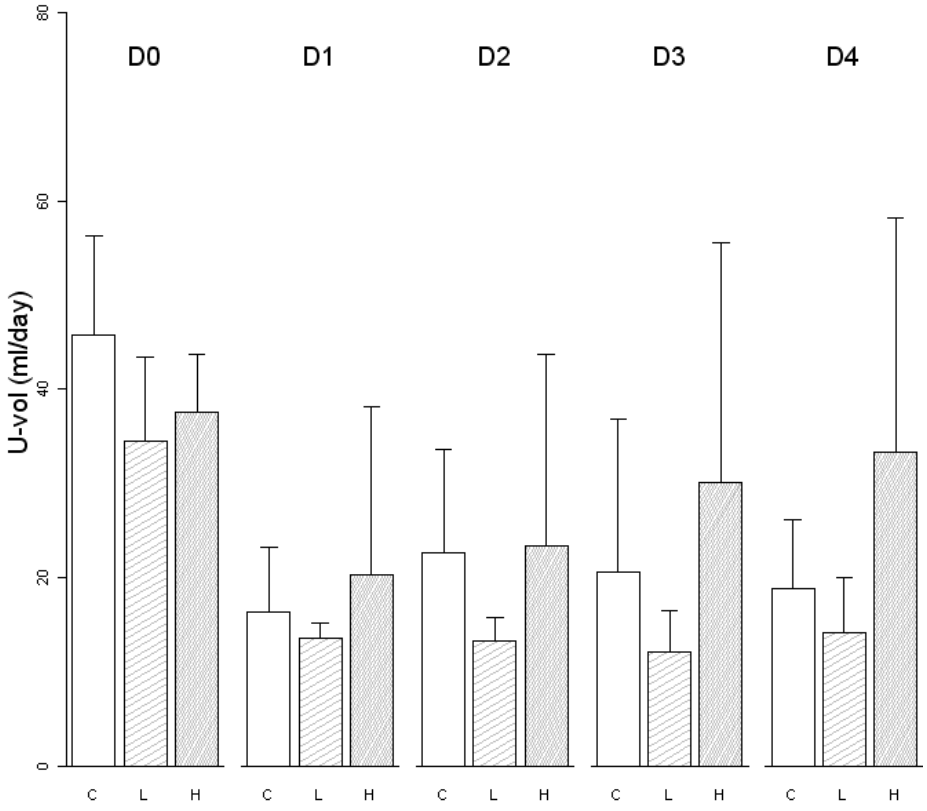

Figure 5. Mean urine volume (U-vol) for three groups of rat during AA dosing. Daily group mean urine volume was compared with the mean urine volume of control group at the same day. The mean U-vol of the two dosed groups was not significantly different from the control group ($p > 0.05$, paired t-test). Error bars are the standard deviation of group means.

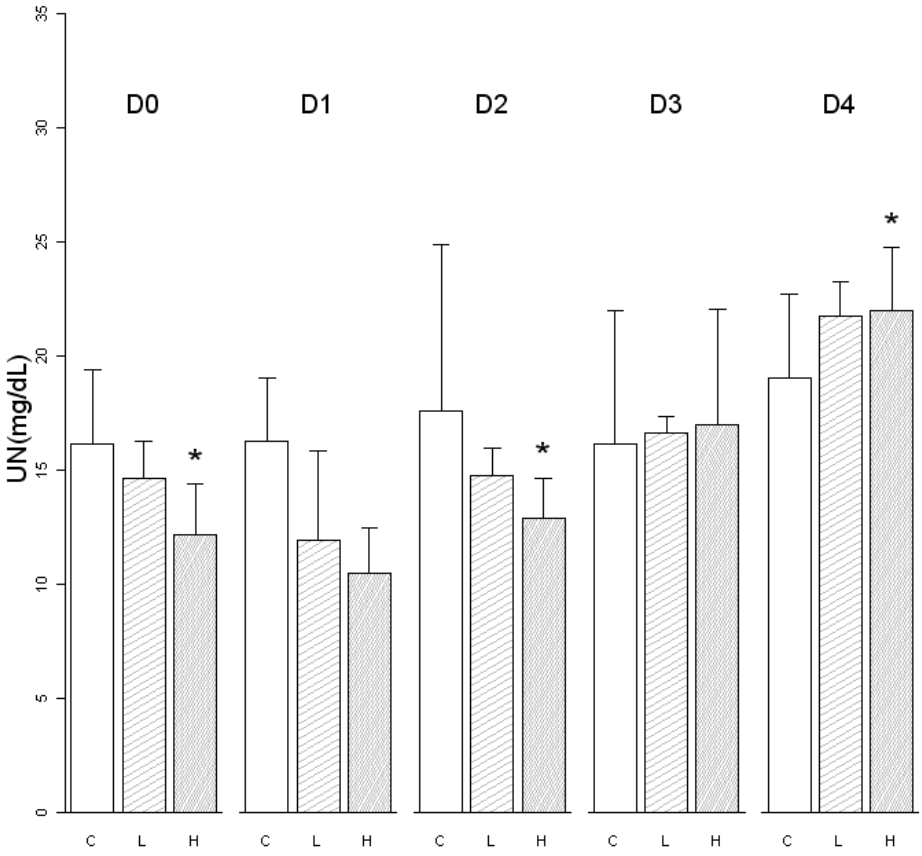

Figure 6. Mean serum urea (UN) for three groups of rat in AA experiment. UN of high dose groups on day 0, 2, 4 (D0, D2 and D4) was significant different from their respective group mean at day 1 (D1). Error bars are the standard deviation of group means. (* $p < 0.05$, paired t test).

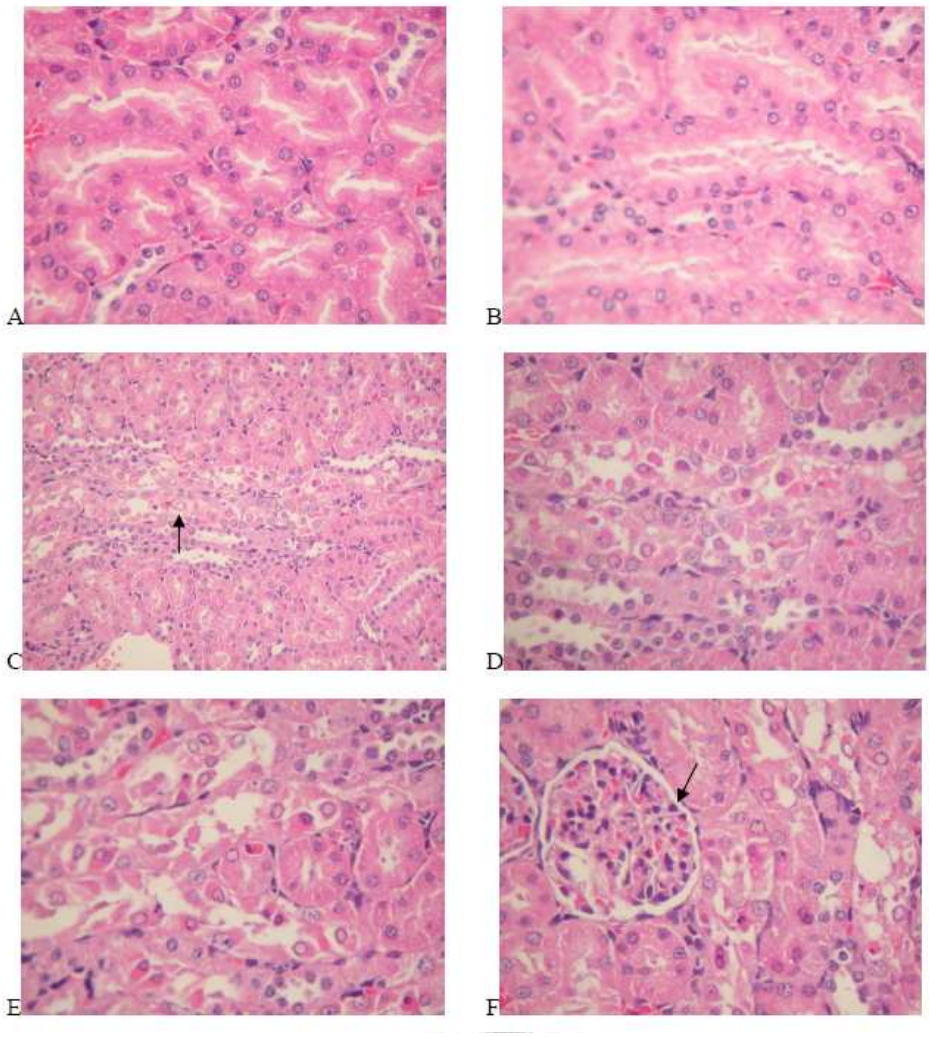

Figure 7. Renal histopathological findings in the rat AA experiment. Normal architecture of kidney in No. 1 rat of control group (A and B. 400x). A pattern of acute proximal renal tubular necrosis (arrow) was note in high dose AA group rats (C. 100x, D. 200x, E. 400x). No morphological change was noted in the glomerulus (arrow) (F. 400x). H&E stain.

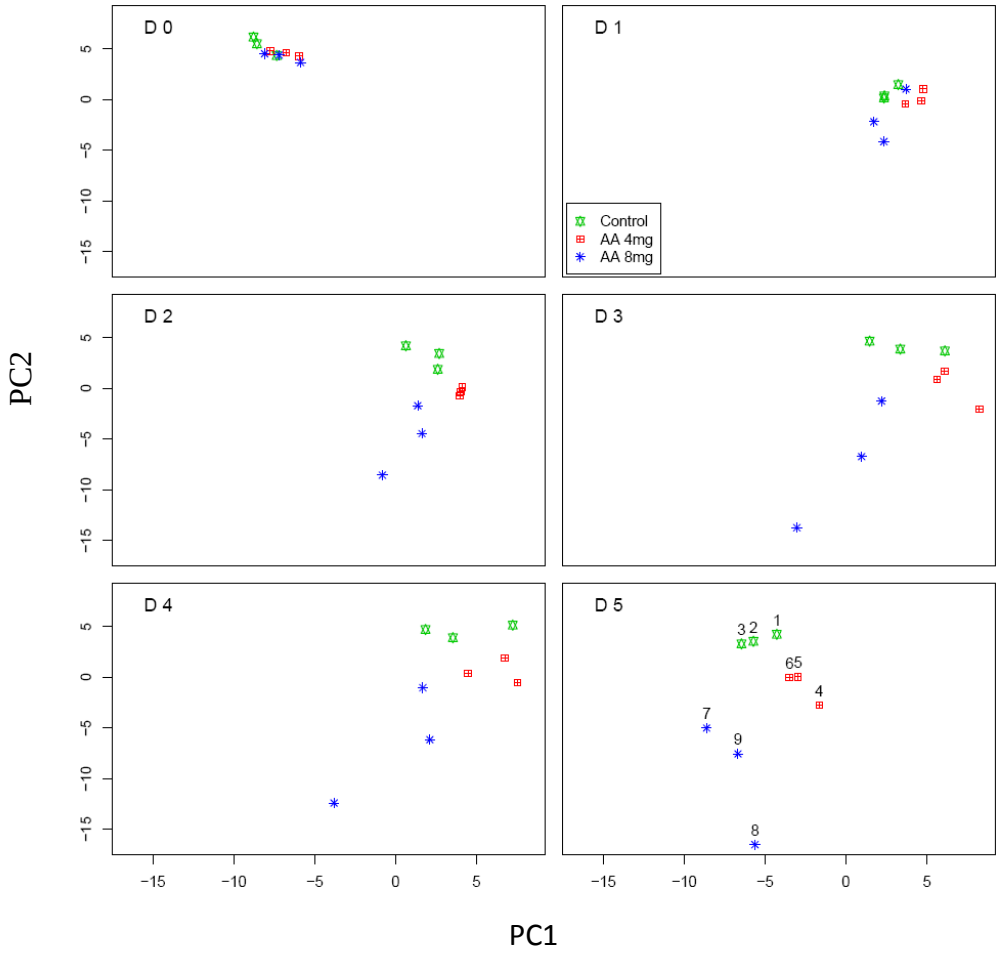

Figure 8. PCA scoring plots of rat urine NMR spectra showed daily change before and after AA standard exposure. All 3 groups clustered together on day 0 under fasting status. Control, low dose (4 mg/day) and high dose (8 mg/day) groups were clustered separately from day 2 (D2) to day 5 (D5). The labels in day 5 was the individual urine sample, 1-3: control, 4-6: low dose and 7-9: high dose group. The x-axis of all plots was the value of PC1 and y-axis PC2. The sum of PC1 and PC2 is 26.2%.

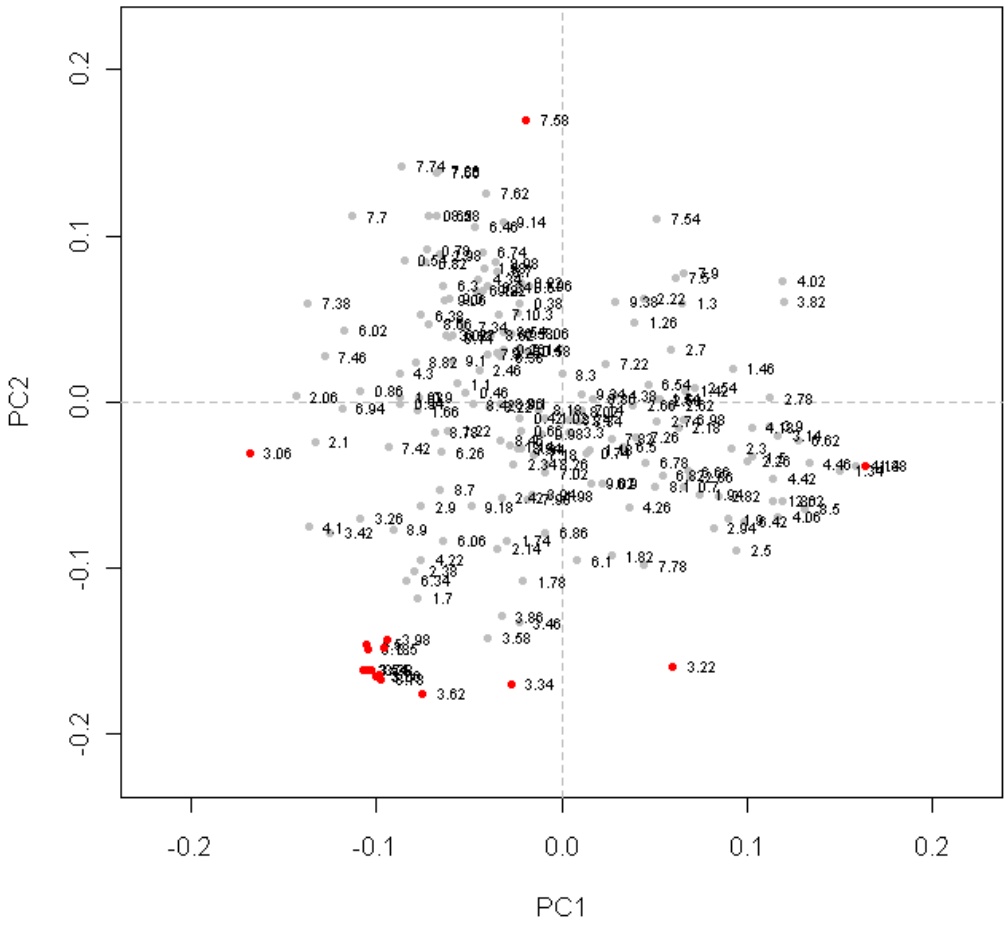

Figure 9. Loading plot of rat urine NMR spectra. Several variables were significantly deviated from the center with Euclidean distance ($p<0.05$). Their binned ppm values were 1.38, 3.06, 3.18, 3.22, 3.34, 3.38, 3.50, 3.54, 3.62, 3.66, 3.70, 3.74, 3.78, 3.98, 4.50 and 7.58.

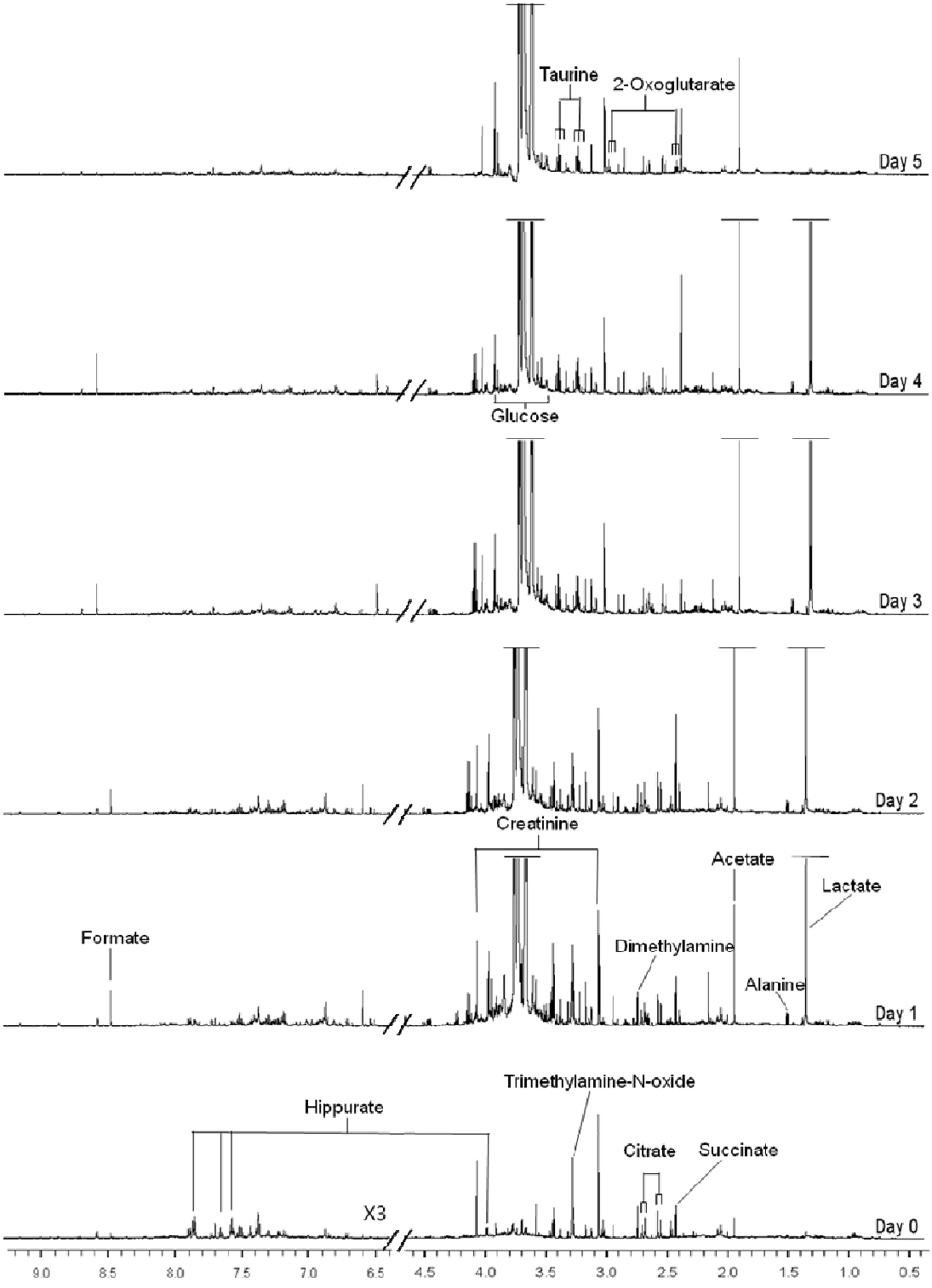

Figure 10. Representative urine NMR spectra of a rat in the high dose AA group.

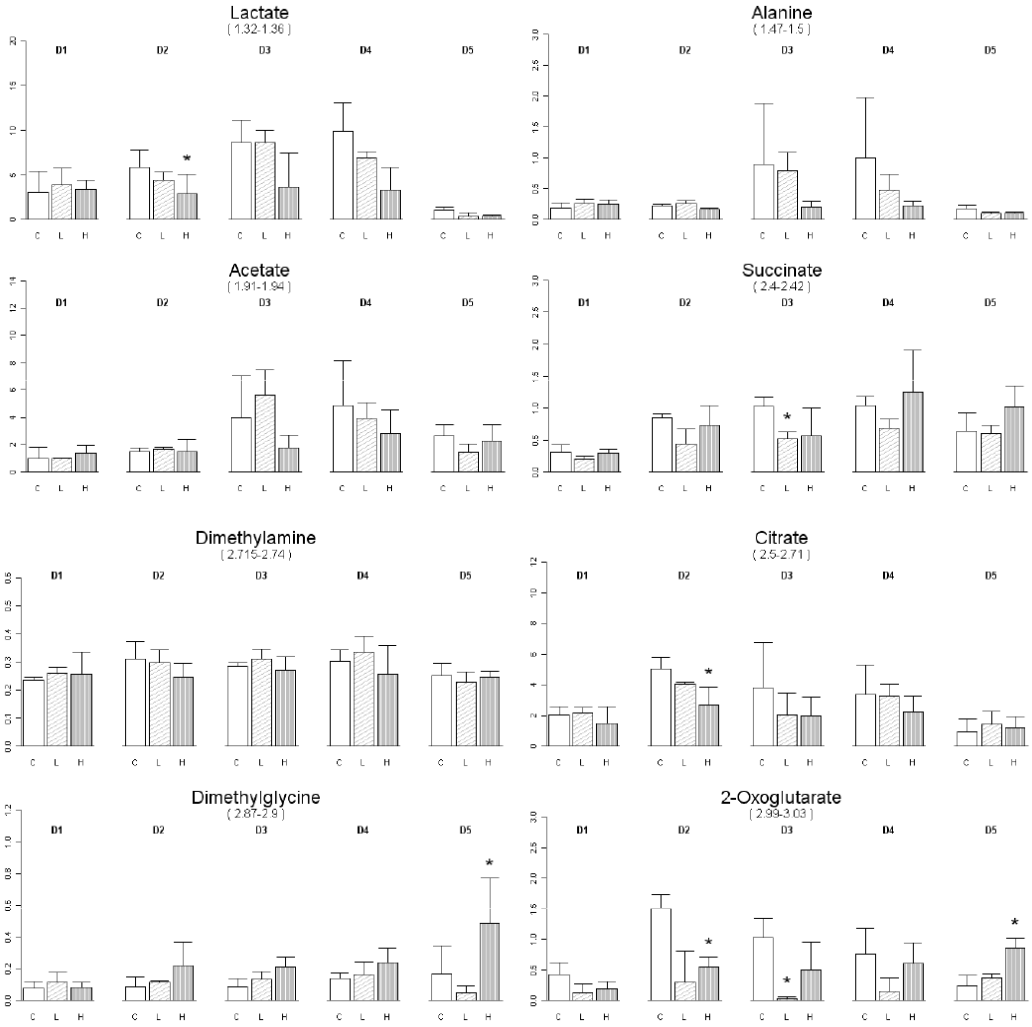

Figure 11. Relative concentration ratio of assigned metabolites to creatinine in rat AA experiment. Each standard deviation bar is the mean of metabolite concentration of the same dosed group (C: control, L: low and H: high) on the same day from day 1 (D1) to day 5 (D5). Student paired t-test was used for estimating significant difference between control and either low or high dosed group at the same day. Parenthesis below the name of metabolites denotes the chemical shifts range for integration. Here shows several metabolites within 1.32 to 3.03 ppm. * $p < 0.05$.

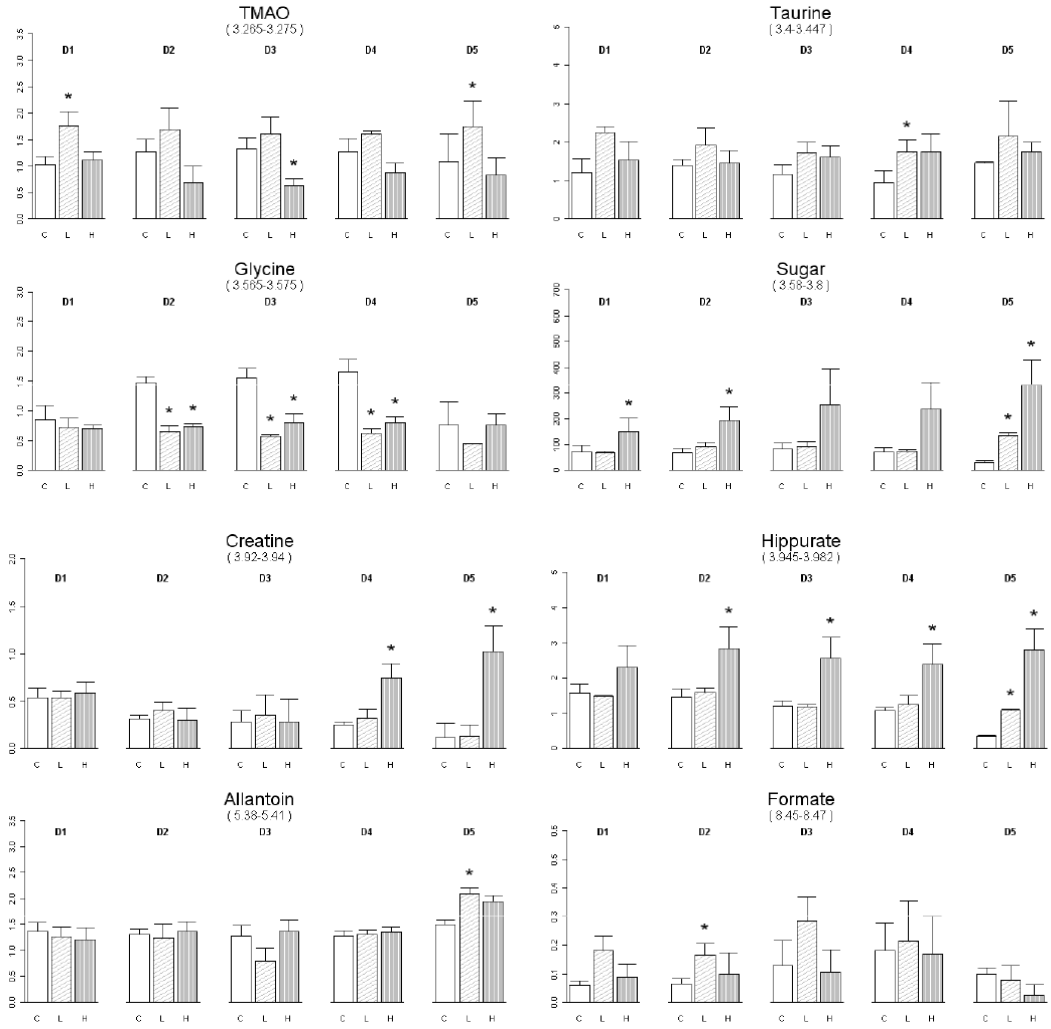

Figure 11 (continued). Metabolite concentration changes for assigned endogenous metabolites with 3.26 and 8.45 ppm.

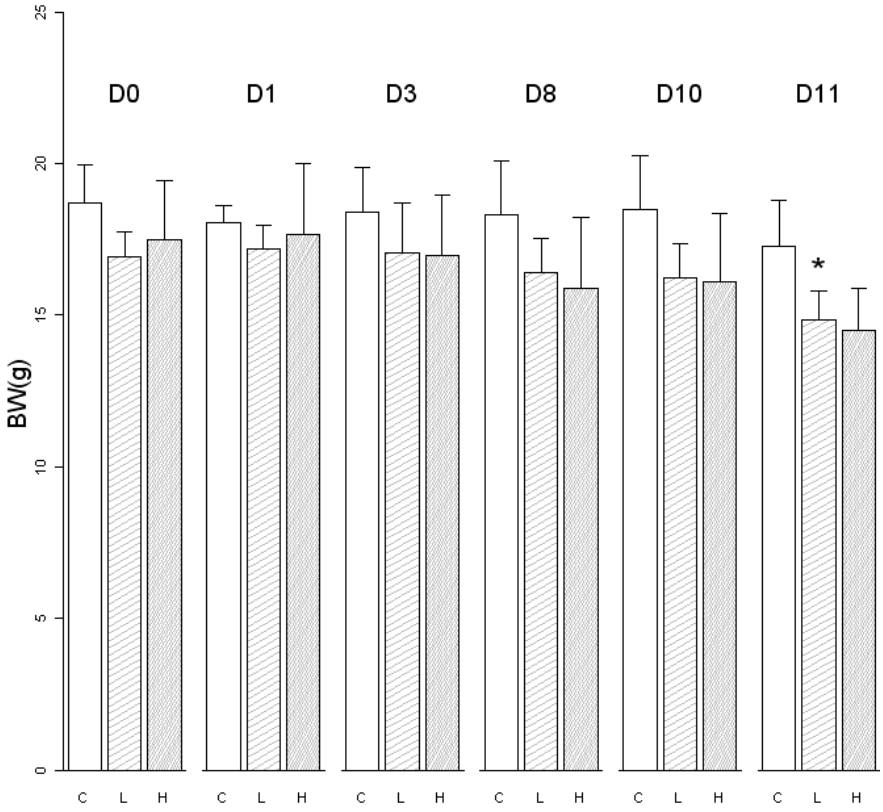

Figure 12. Mean body weight (BW) changes in three groups of mouse in AA experiment. The group mean BW of each day was tested with that at day 0 (D0) of the same group. * $p < 0.05$, t-test. C: control (n=3), L: low (n=3), H: high (n=4 D0-D8, n=3 at D10 and D11) dose group.

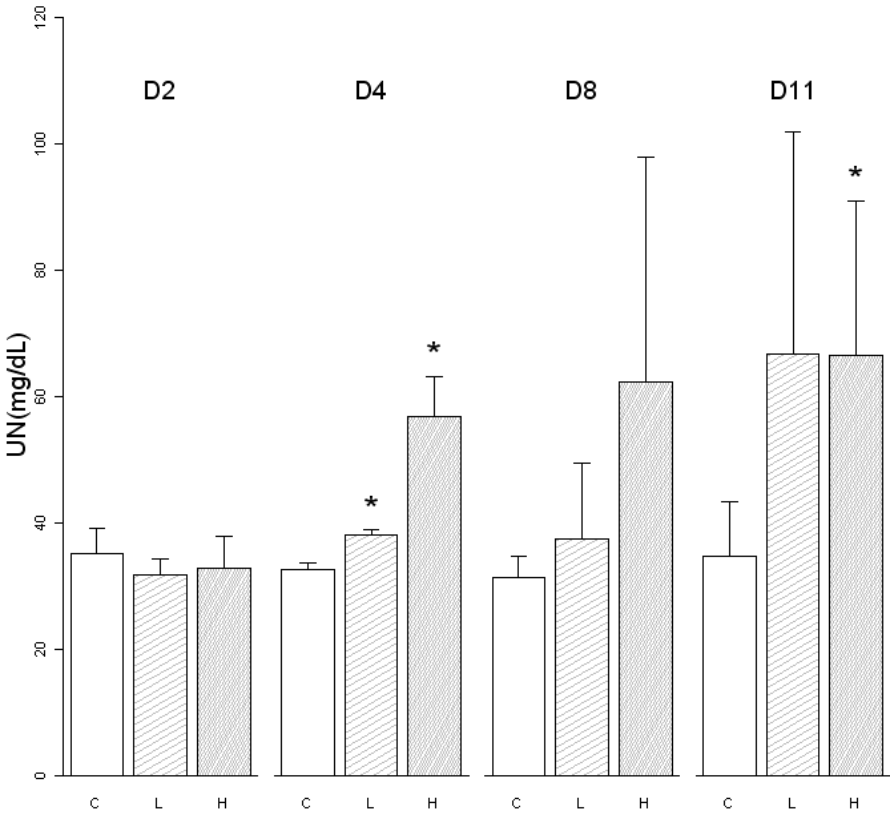

Figure 13. Mean serum urea (UN) for three groups of mouse in AA experiment. Mean UN of each group at Day 4, 8 and 11 was compared with day 2 of the same group. * $p < 0.05$, t-test. Mouse groups were C: control (n=3), L: low (n=3), H: high (n=4 D2, 4 and 8, n=3 at D11).

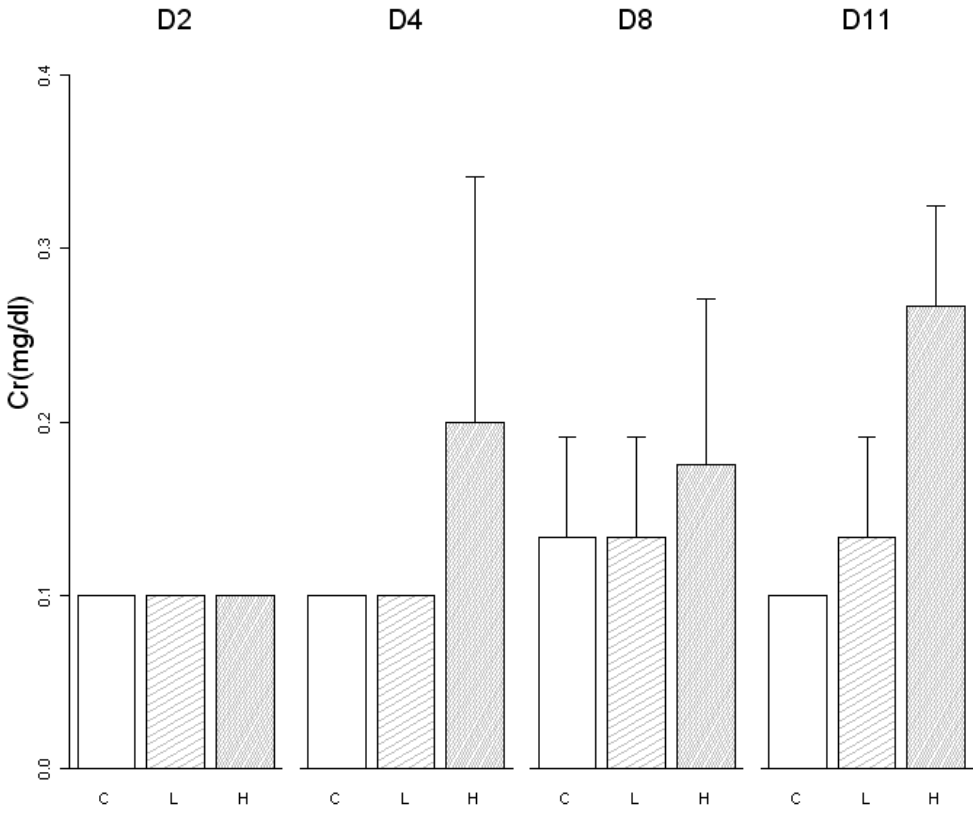

Figure 14. Mean serum creatinine (Cr) for three groups of mouse in AA experiment. Cr of the high dose group increased more from day 4 (D4) to day 11 (D11) than other groups. Mouse groups were C: control (n=3), L: low (n=3), H: high (n=4 D2, 4 and 8, n=3 at D11).

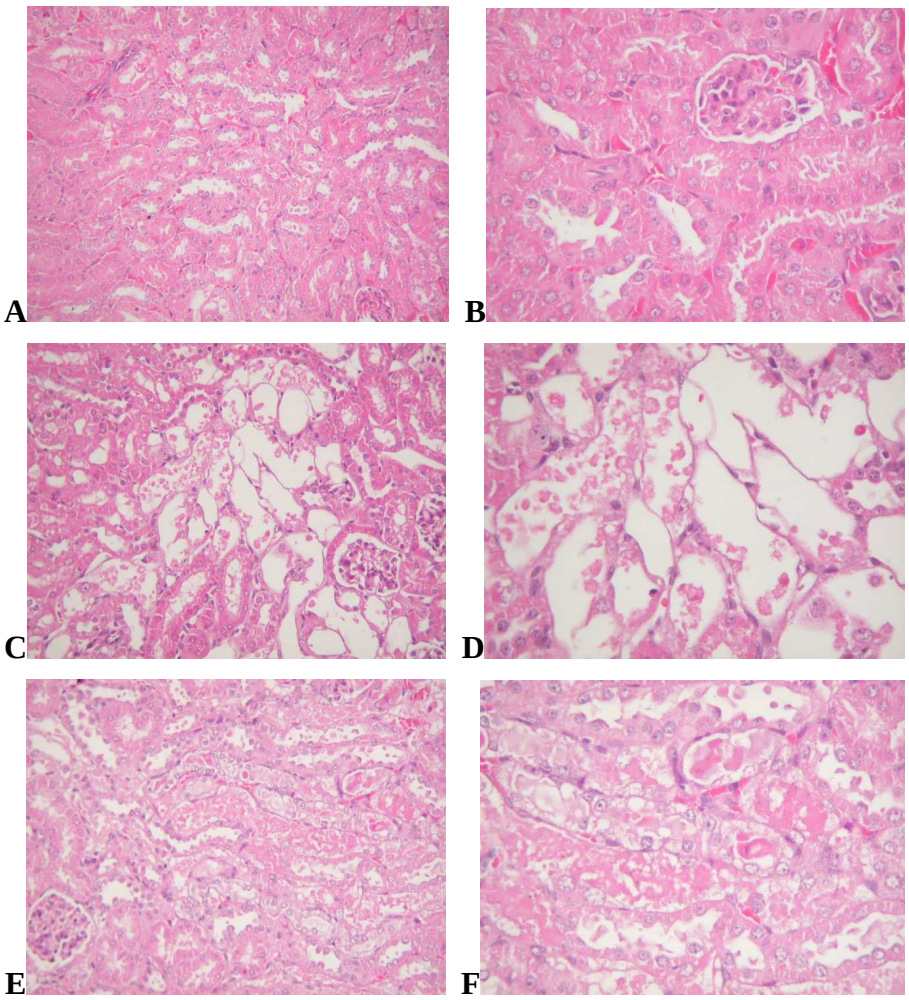

Figure 15. Histopathological findings of mouse kidneys dosed with AA standard. No significant change of renal tubules and glomeruli of kidney in a mouse of control group (A. 200x, B. 400x). A mouse of low dose AA (5 mg/kg/day) group showed focal moderate (3) to severe acute proximal tubular necrosis and dilation with hyaline casts (C. 200x, D. 400x). A mouse of high dose AA (7.5 mg/kg/day) group showed focal moderately severe (4) acute proximal tubular necrosis with hyaline casts (E. 200x, F. 400x). No morphological change was noted in the glomeruli. H&E stain.

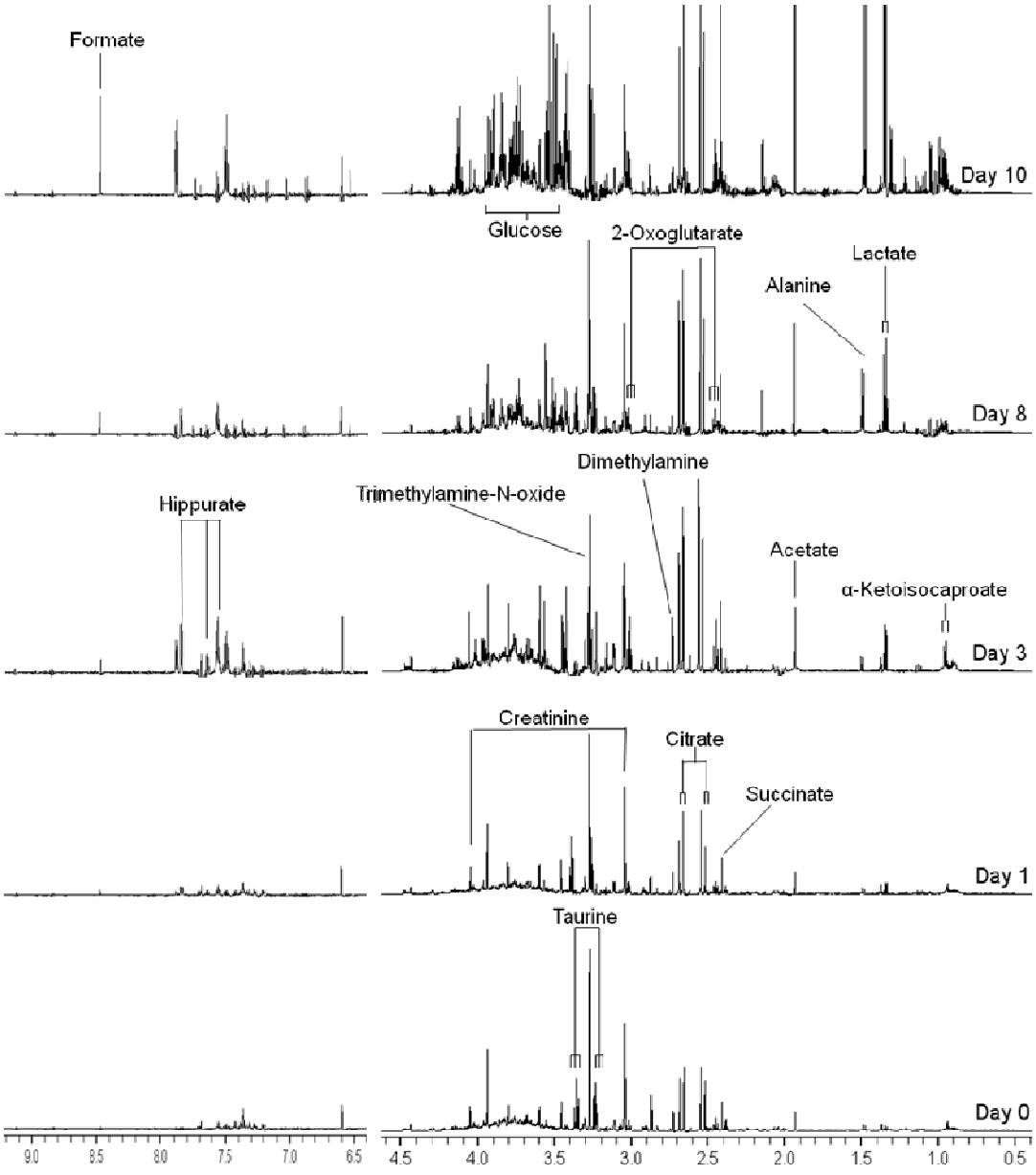

Figure 16. Representative urine NMR spectra of a mouse from the high dose AA group.

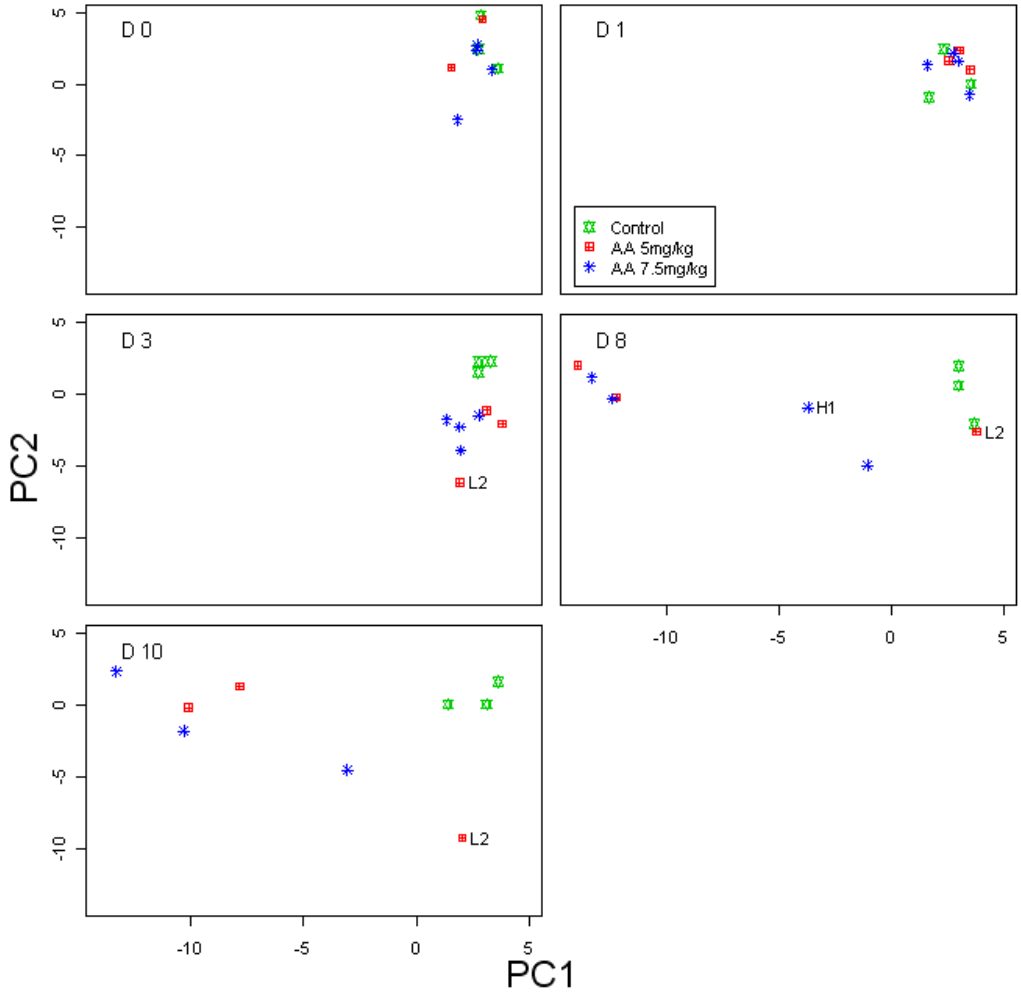

Figure 17. PCA scoring plots of mouse urine NMR spectra showed clustering before and after AA standard exposure in the mouse AA experiment. The chemical shifts range selected was from 1 to 4.5 ppm. The control group and the dose groups were clustered separately at day 3 and later except a mouse of the low dose group labeled "L2" at day 8. There was no urine sample at D10 for a mouse of high dosed group labeled "H1". The x-axis of all plots was the value of PC1 and y-axis PC2. The sum of PC1 and PC2 is 43.7%.

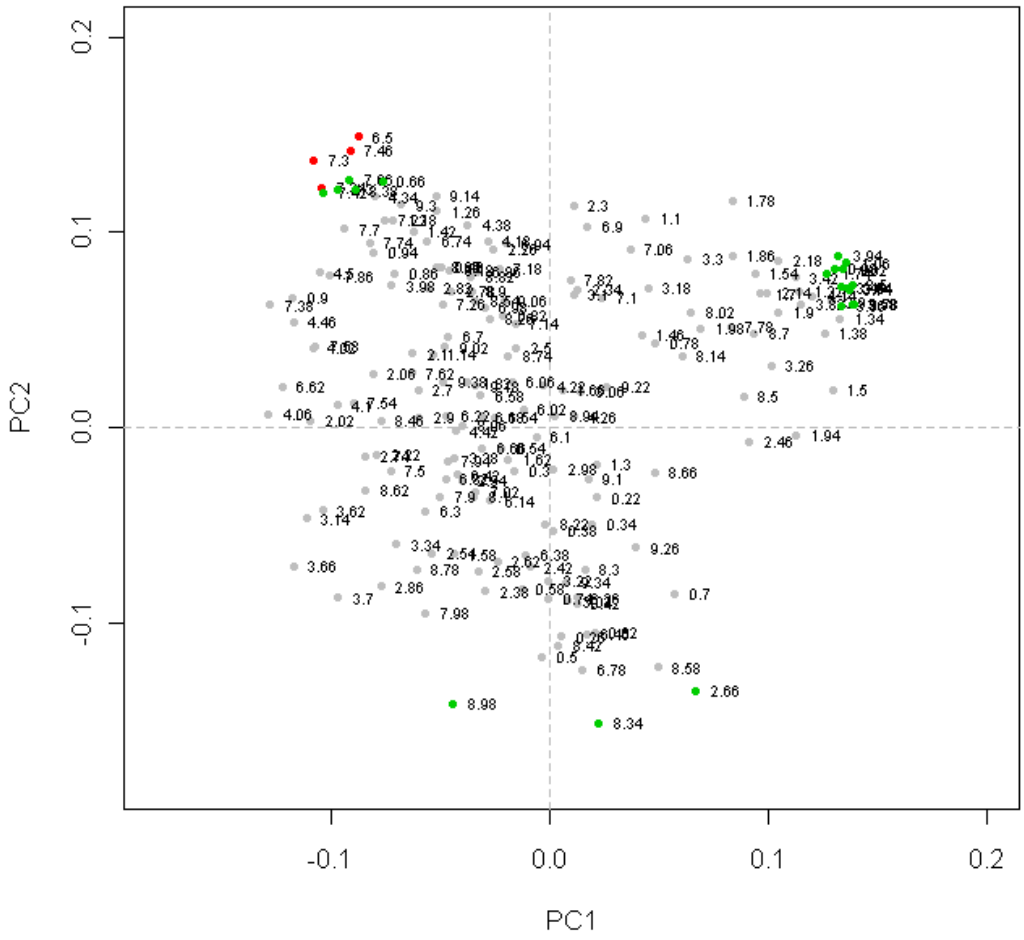

Figure 18. Loading plot of mouse urine NMR spectra of the AA experiment. Several variables were significantly deviated from the center with Euclidean distance ($p < 0.1$, green; $p < 0.05$, red). Their binned ppm values were 0.66, 0.98, 1.02, 1.06, 1.74, 2.66, 3.46, 3.50, 3.54, 3.58, 3.74, 3.78, 3.86, 3.94, 4.30, 7.42, 7.66, 8.34, 8.38 and 8.98.

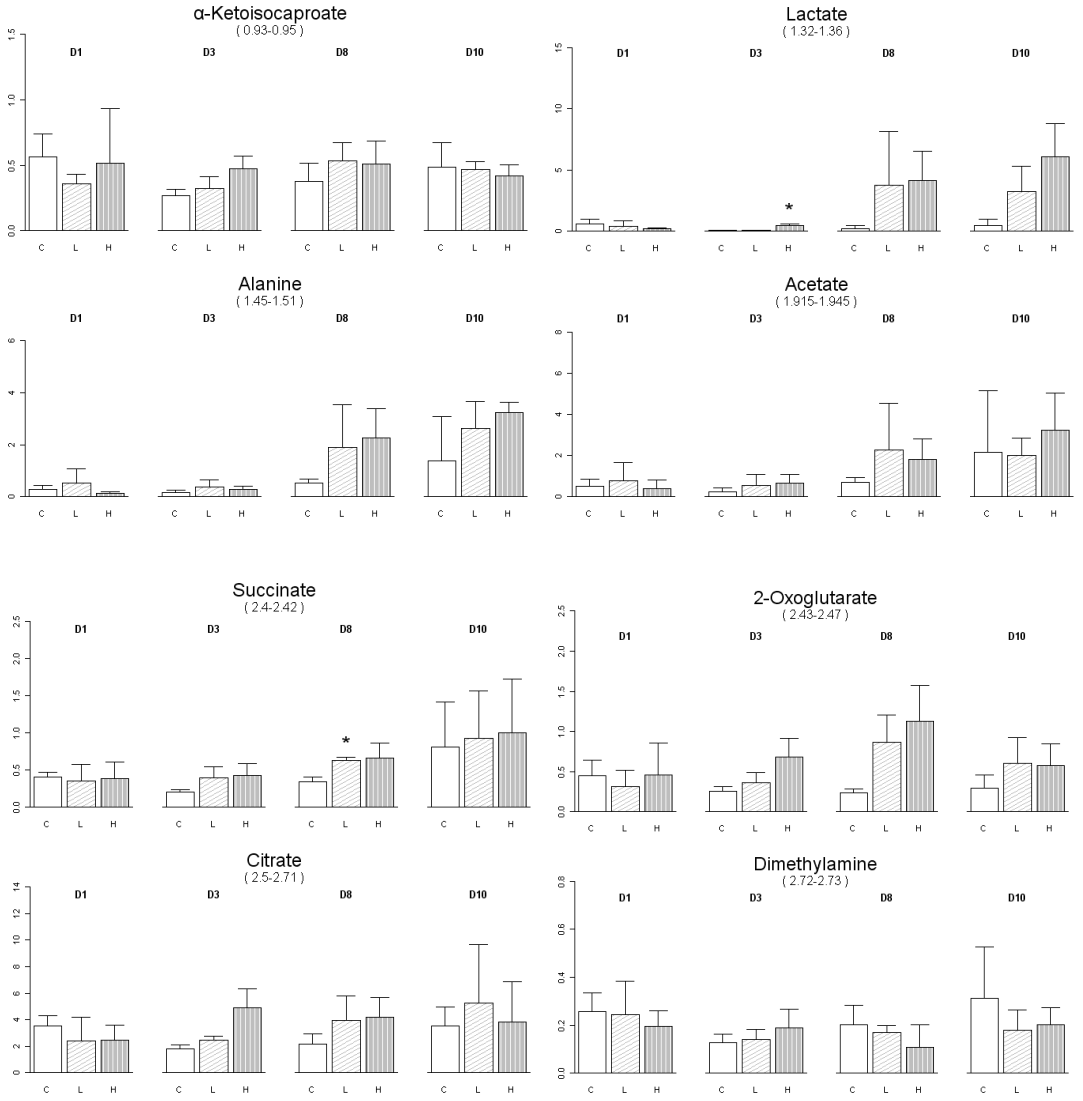

Figure 19. Major endogenous metabolites profile in the mouse AA experiment. Relative concentration ratio of assigned metabolites to creatinine. Each standard deviation bar is the mean of metabolite concentration of the same dosed group (C: control, L: low (5 mg/kg/day) and H: high (7.5 mg/kg/day)) on the same day from day 1 (D1) to day 10 (D10). Parenthesis below the name of metabolites denotes the chemical shifts range for integration. * $p < 0.05$.

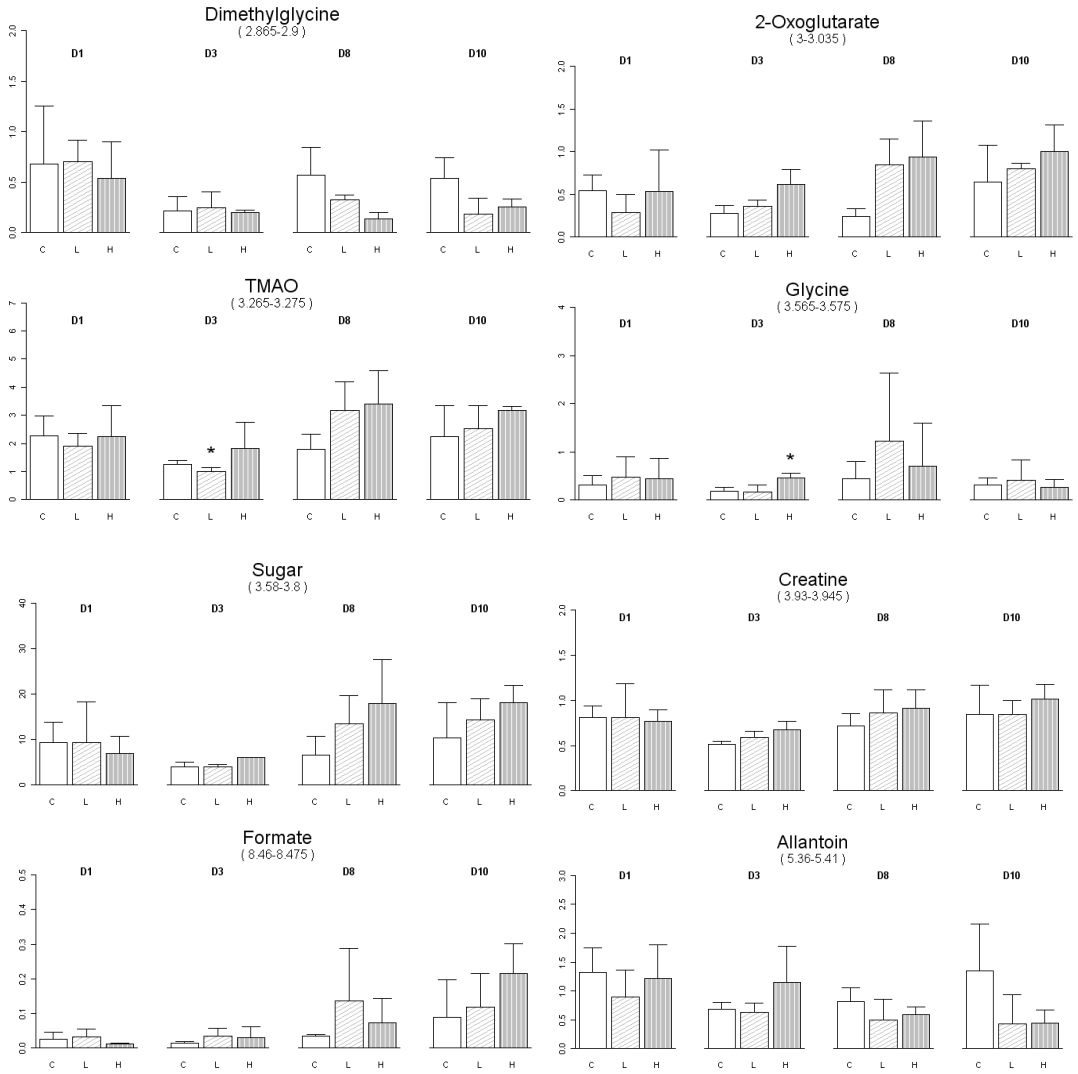

Figure 19 (continued). Metabolite concentration changes among three groups of mouse dosed with AA.

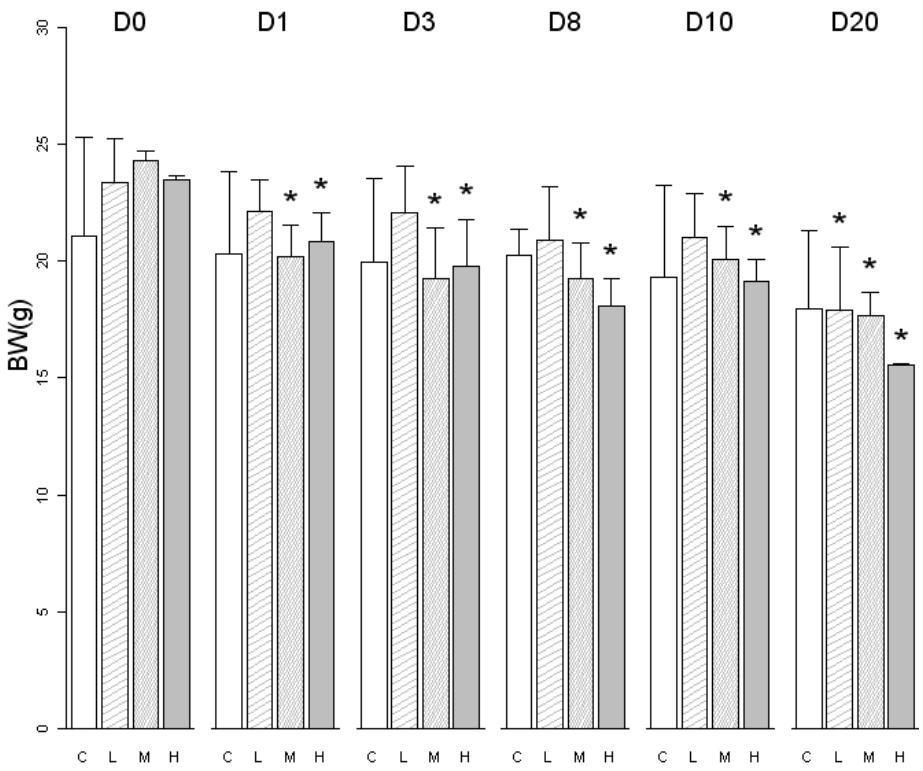

Figure 20. Mean body weight (BW) changes in groups of mouse dosed with Madouling. C: control, L: low (559 mg/kg/day), M: moderate (1118 mg/kg/day), H: high (2236 mg/kg/day). Each mean BW of the same group at different day was compared with its mean BW at day 0 (D0).

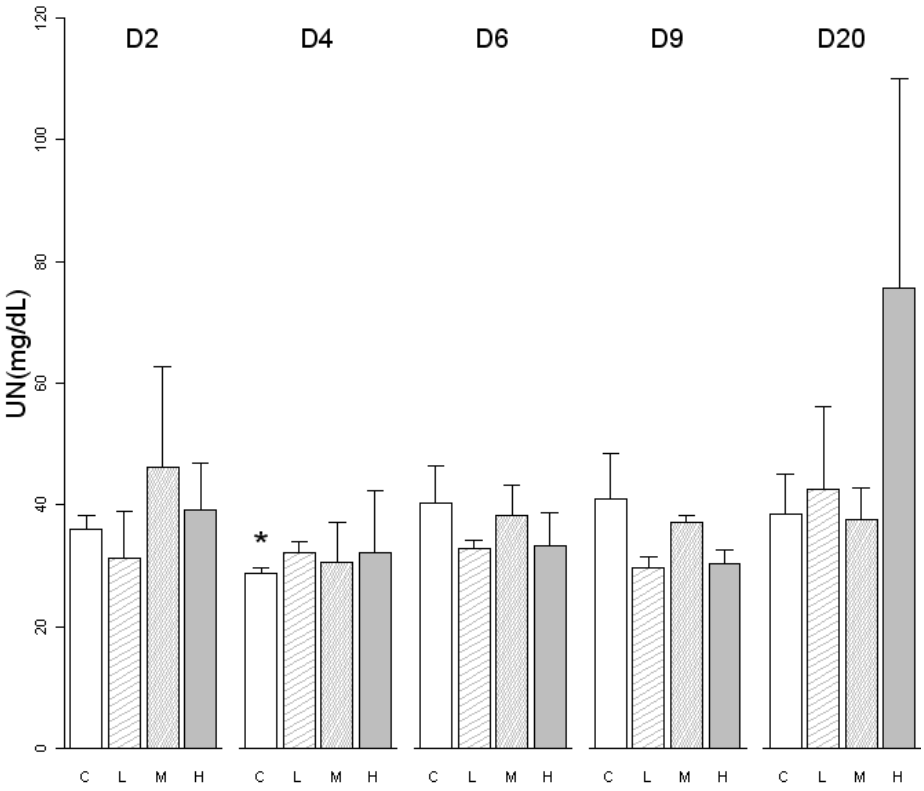

Figure 21. Mean serum urea (UN) for groups of mouse in Madouling experiment. Each mean BW of the same group at different day was compared with its mean UN at day 0 (D0). UN was not increased in all group until day 20 (D20) in the high dose group. There were 3 mice for each group and UN of one mouse in the high dose group was not detected at 9 and day 20 due to mortality. * $p < 0.05$, t-test.

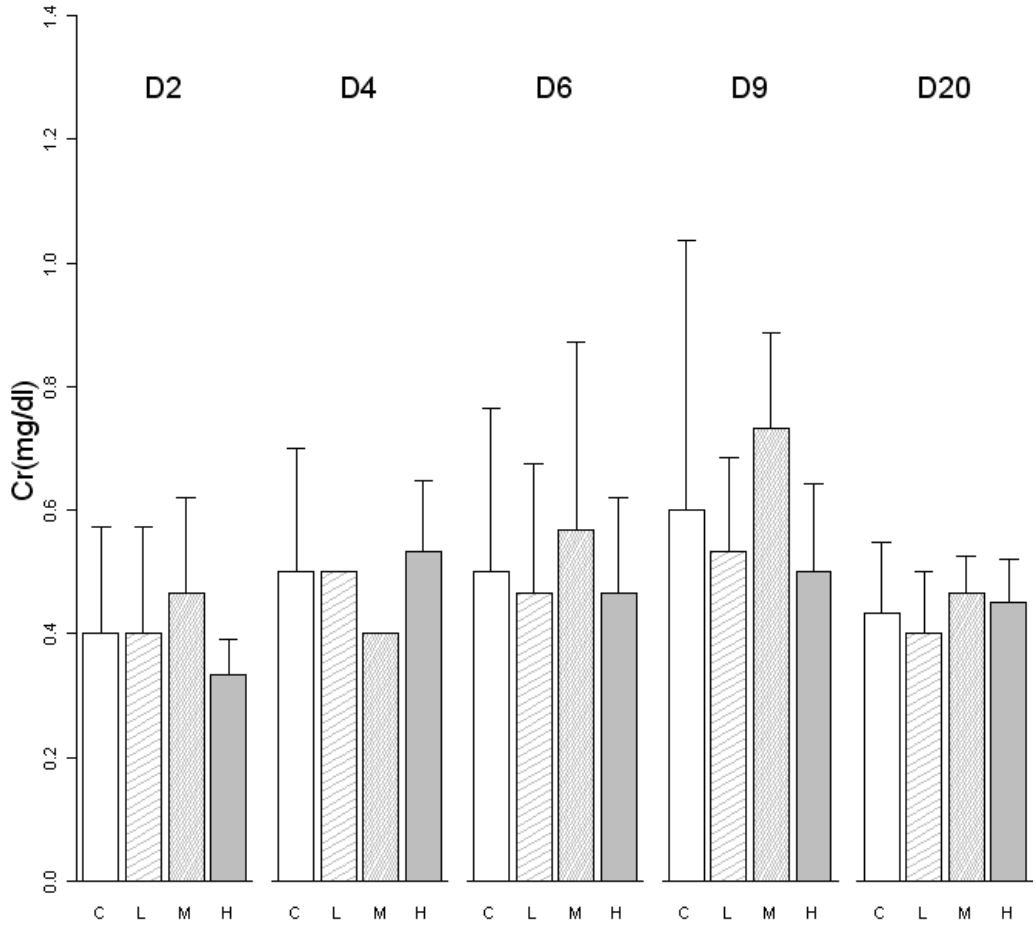

Figure 22. Mean serum creatinine (Cr) for four groups of mouse in Madouling experiment. No difference of mean Cr change for each day creatinine as compared to day 0 of the same group. Mouse groups were C: control (n=3), M: moderate (n=3),L: low (n=3), H: high (n=3 D2, 4 and 6, n=2 at D9 and D20).

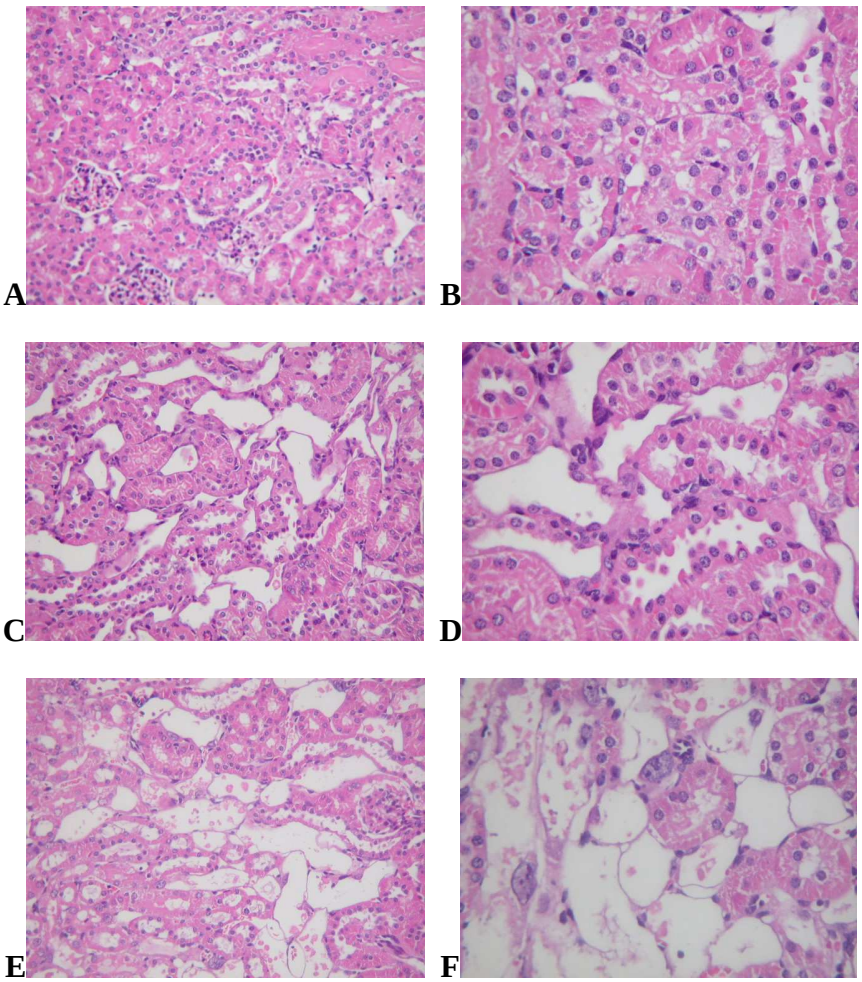

Figure 23. Histopathological findings of mouse kidneys dosed with Madouling at day 20. A mouse of low dose (559 mg/kg/day) group showed focal slight acute proximal tubular degeneration with cellular swelling (A. 200x, B. 400x). The moderate dose (1118 mg/kg/day) group showed focal moderate acute proximal tubular necrosis with dilation (C. 200x, D. 400x). The high dose (2236 mg/kg/day) group showed focal moderate/serve acute proximal tubular necrosis with dilation (E. 200x, F. 400x). No morphological change was noted in the glomerulus. H&E stain.

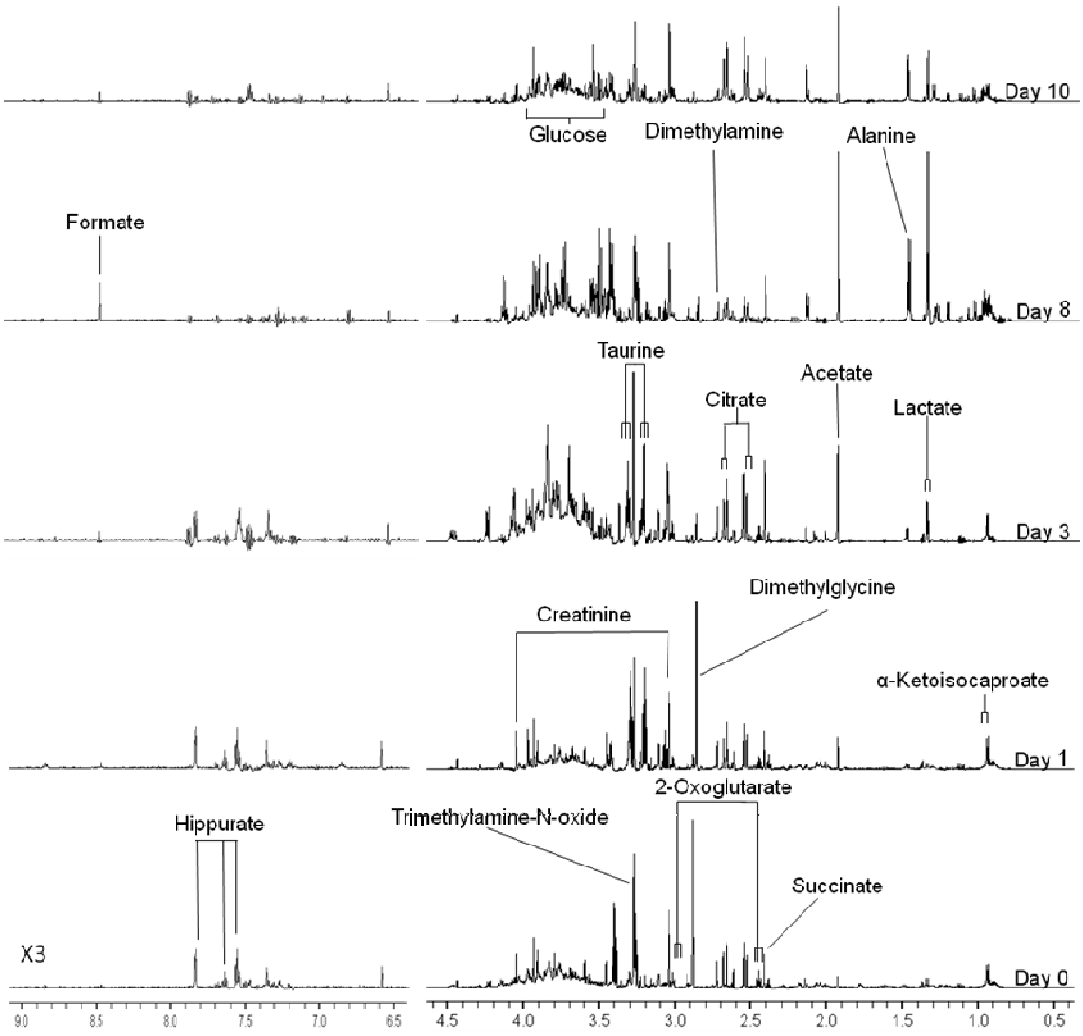

Figure 24. Representative urine NMR spectra of a mouse of high dose (2236 mg/kg/day) group in the Madouling experiment.

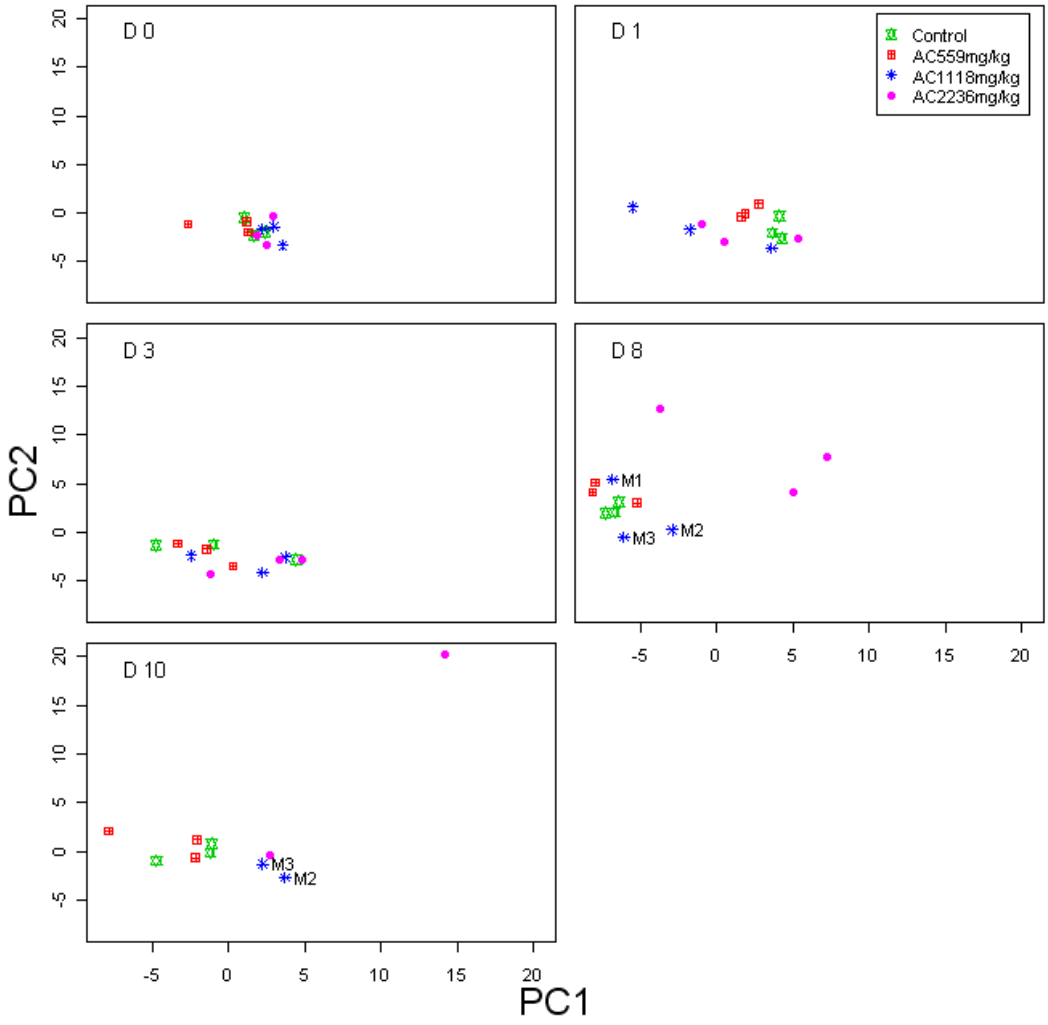

Figure 25. PCA scoring plots of mouse urine NMR spectra showed daily change before (D0) and after Madouling (AC) exposure. At day 8 (D8), the high dose group showed separation from other groups. At day 10 (D10) the cluster of two dose groups were separated from the control group. Scoring points labeled M1-3 were individual mouse of the moderate dose group. The sum of PC1 and PC2 is 22.6%.

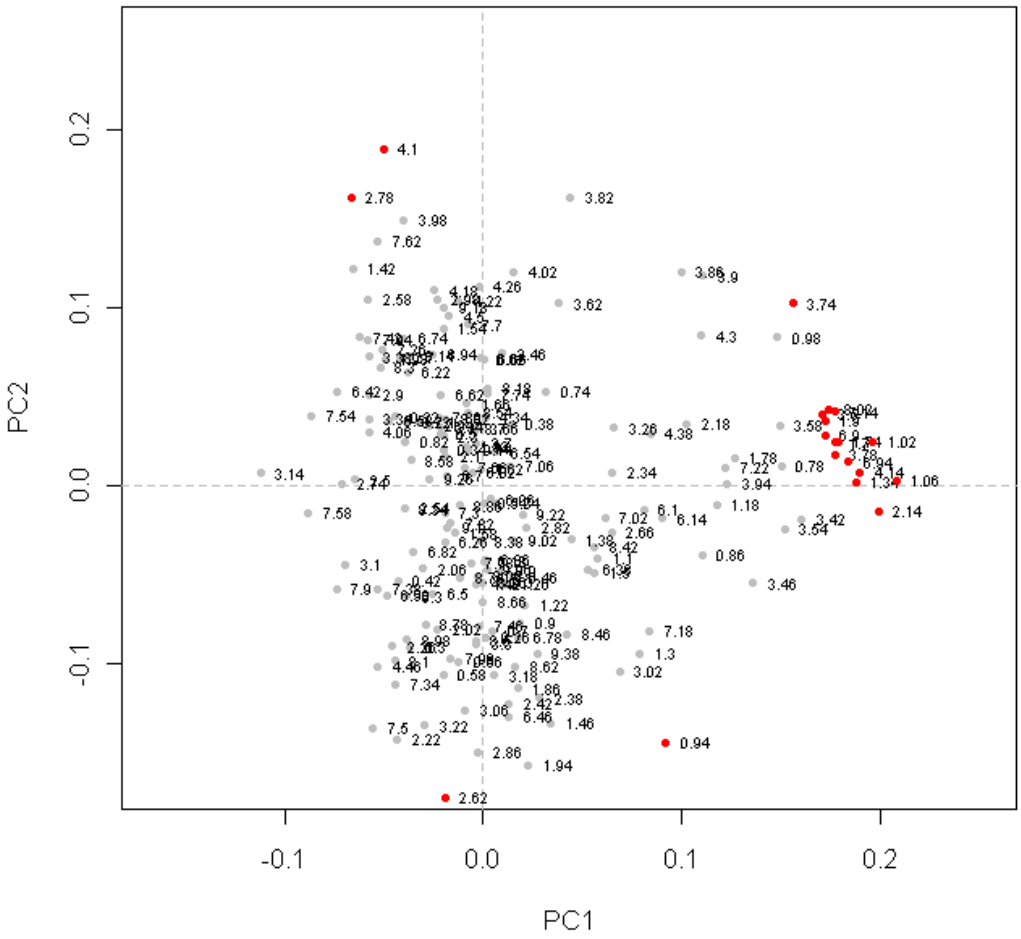

Figure 26. Loading plot of mouse urine NMR spectra in the Madouling experiment. Several variables were significantly deviated from the center with Euclidean distance ($p < 0.05$, red). Their binned ppm values were 0.94, 1.02, 1.06, 1.34, 1.70, 1.74, 1.90, 2.14, 2.62, 2.78, 3.50, 3.74, 3.78, 4.10, 4.14, 6.90, 6.94, 7.14 and 8.02.

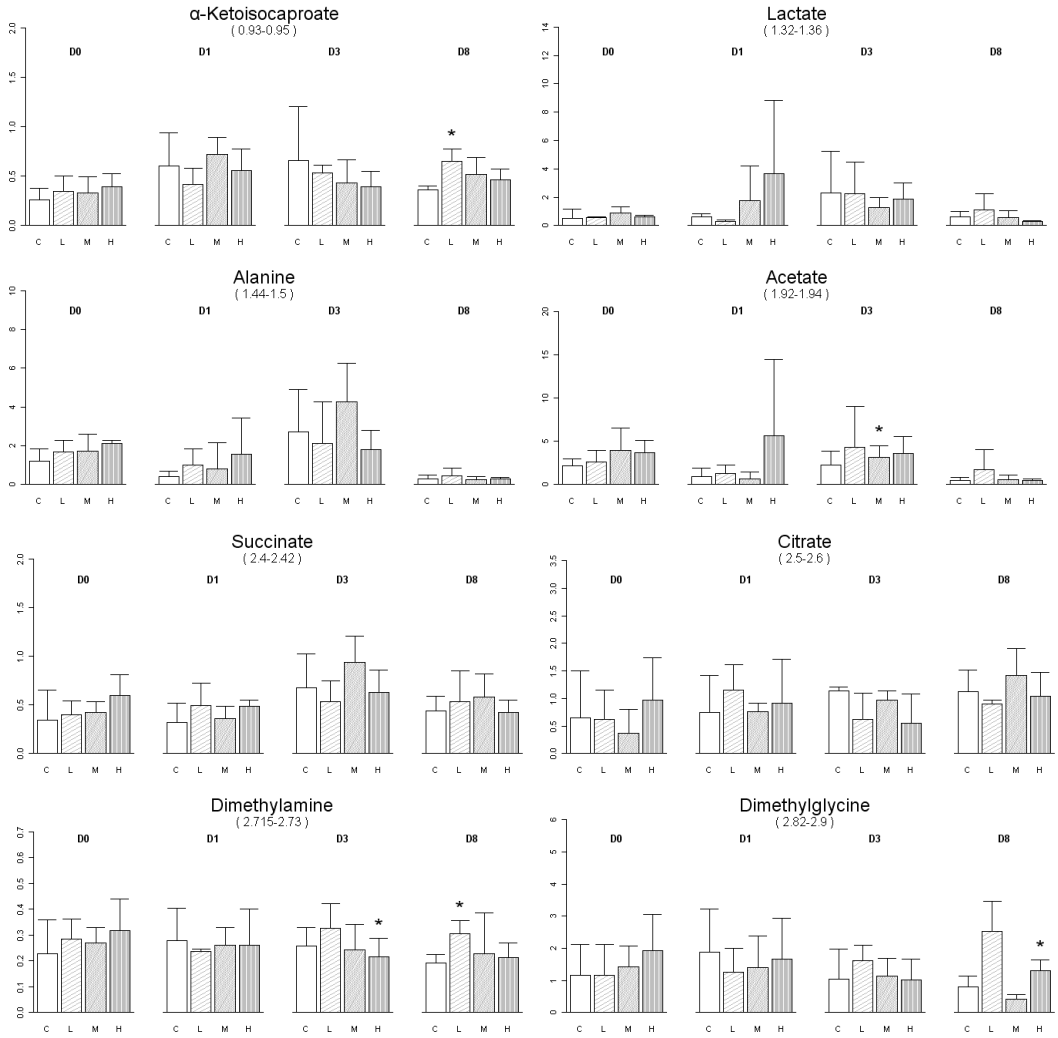

Figure 27. Relative concentration ratio of assigned metabolites to creatinine in the mouse Madouling experiment. Each standard deviation bar is the mean of metabolite concentration of the same dosed group (C: control, L: low (559 mg/kg/day), M: moderate (1118 mg/kg/day) and H: high (2236 mg/kg/day)) at day 0, 1, 3 and 8. Parenthesis below the name of metabolites denotes the chemical shifts range for integration. * $p < 0.05$.

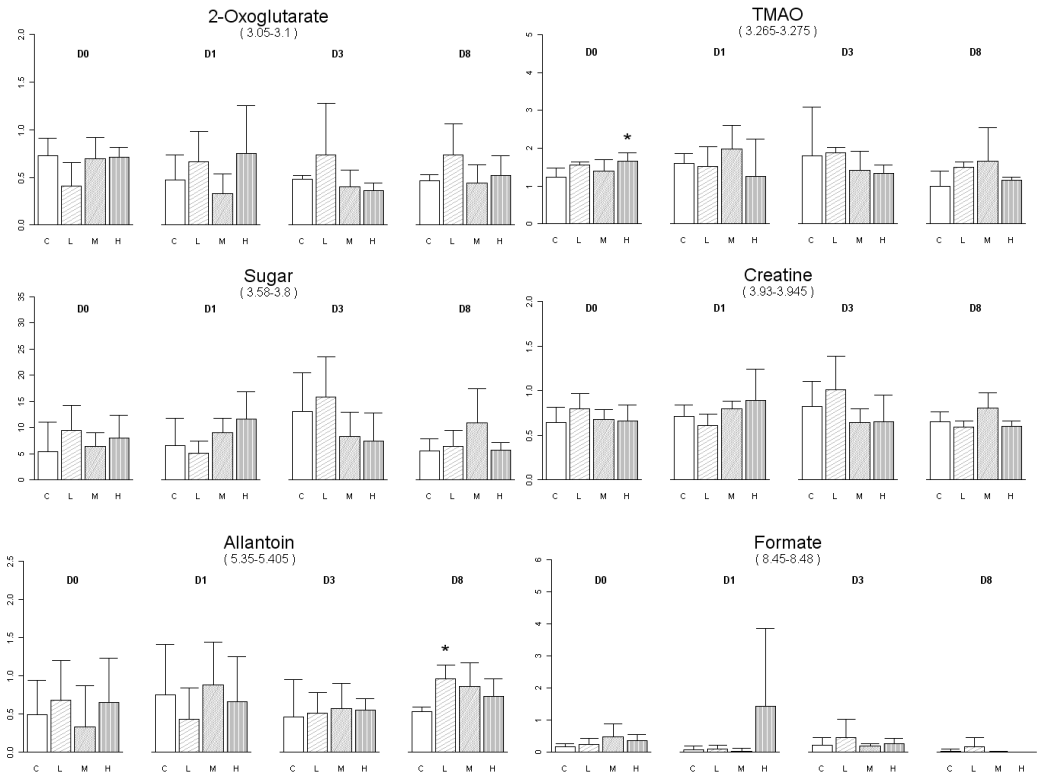

Figure 27 (continued). Metabolite concentration changes among four groups of mouse dosed with Madouling.

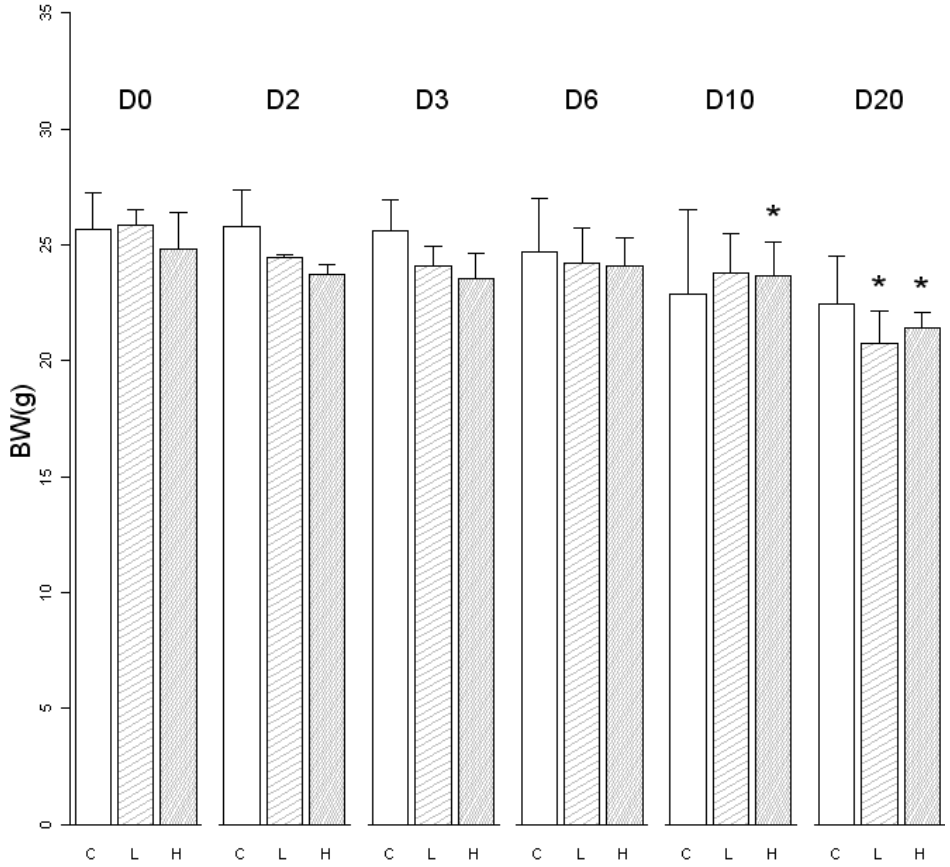

Figure 28. Mean body weight (BW) changes in groups of mouse dosed with Bu-Fei-A-Jiau-Tang (BFAJT). C: control (n=3), L: low (n=3), H: high (n=3). Each group mean BW at different day was compared with day 0 (D0) of the same group. The mean BW was significantly different at day 10 (D10) and day 20 (D20) for high dose (4 g/kg/day) group and at D20 for low dose (2 g/kg/day) group. * $p < 0.05$, paired t-test.

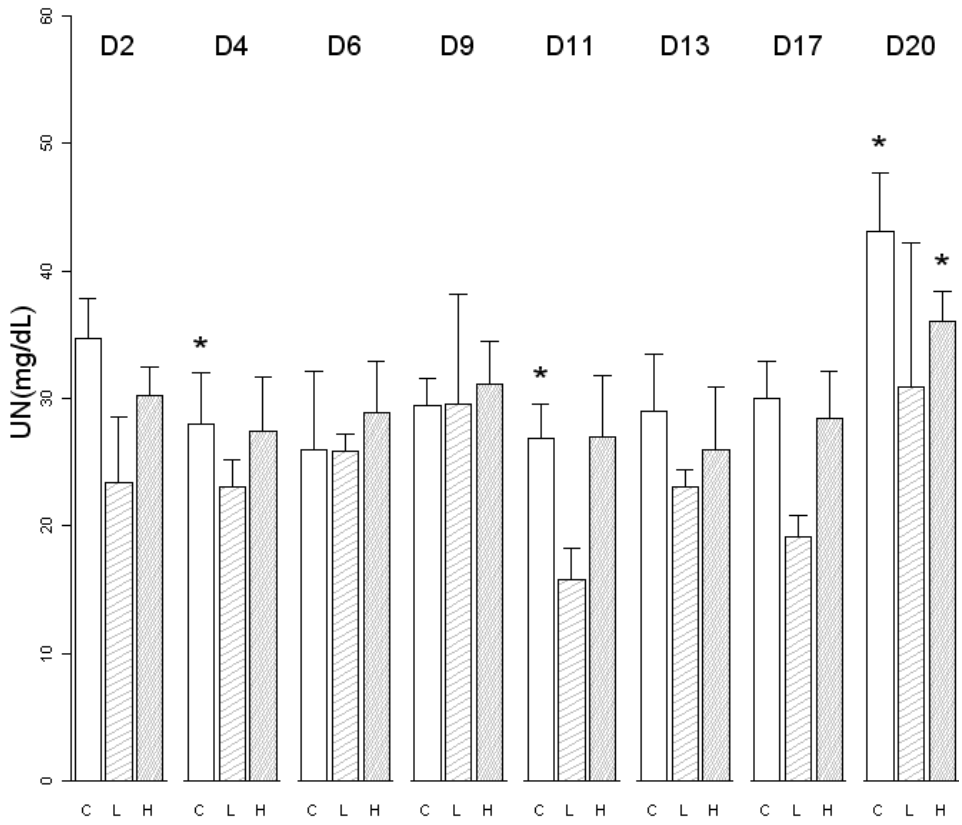

Figure 29. Mean serum urea (UN) for groups of mouse during Bu-Fei-A-Jiau-Tang dosing. The mean UN of high dose group at day 20 (D20) was significantly higher than its mean UN at day 0 (D0). The standard deviation of group means are shown in stick arrows. * $p < 0.05$ as comparing with control group at the same day.

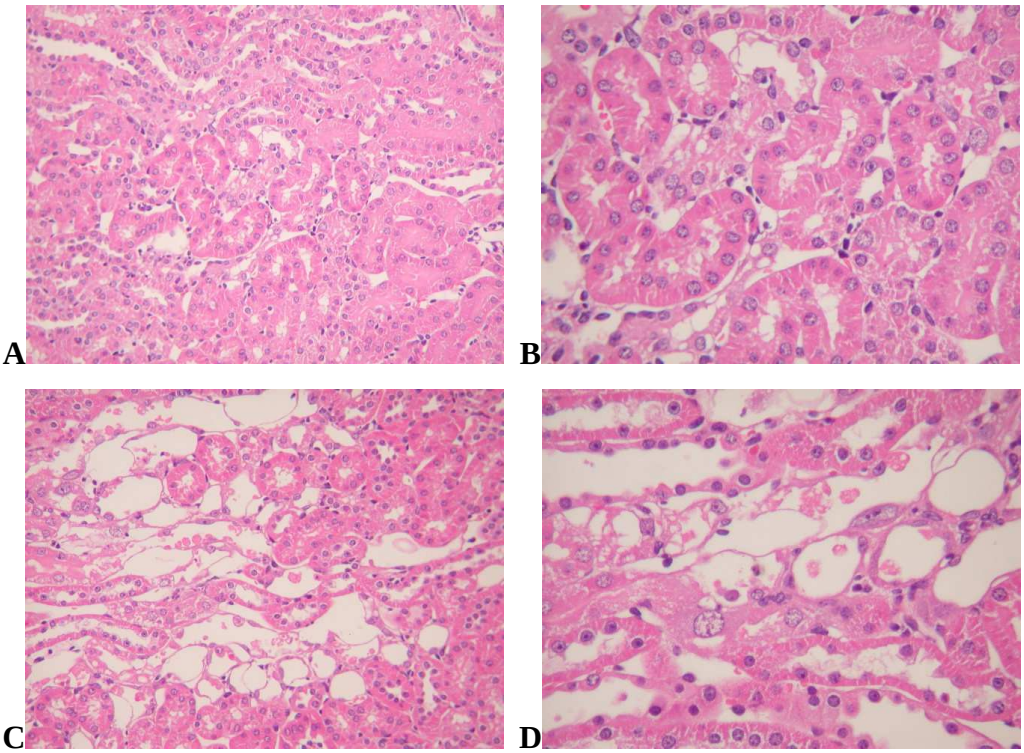

Figure 30. Histopathological findings of mouse kidneys dosed with BFAJT after dosing for 20 days. A mouse of low dose (2 g/kg/day) group showed focal slight acute proximal tubular degeneration with cellular swelling (A. 200x, B. 400x). The high dose (4 g/kg/day) group showed focal moderate acute proximal tubular necrosis with dilation (C. 200x, D. 400x). No morphological change was noted in the glomerulus. H&E stain.

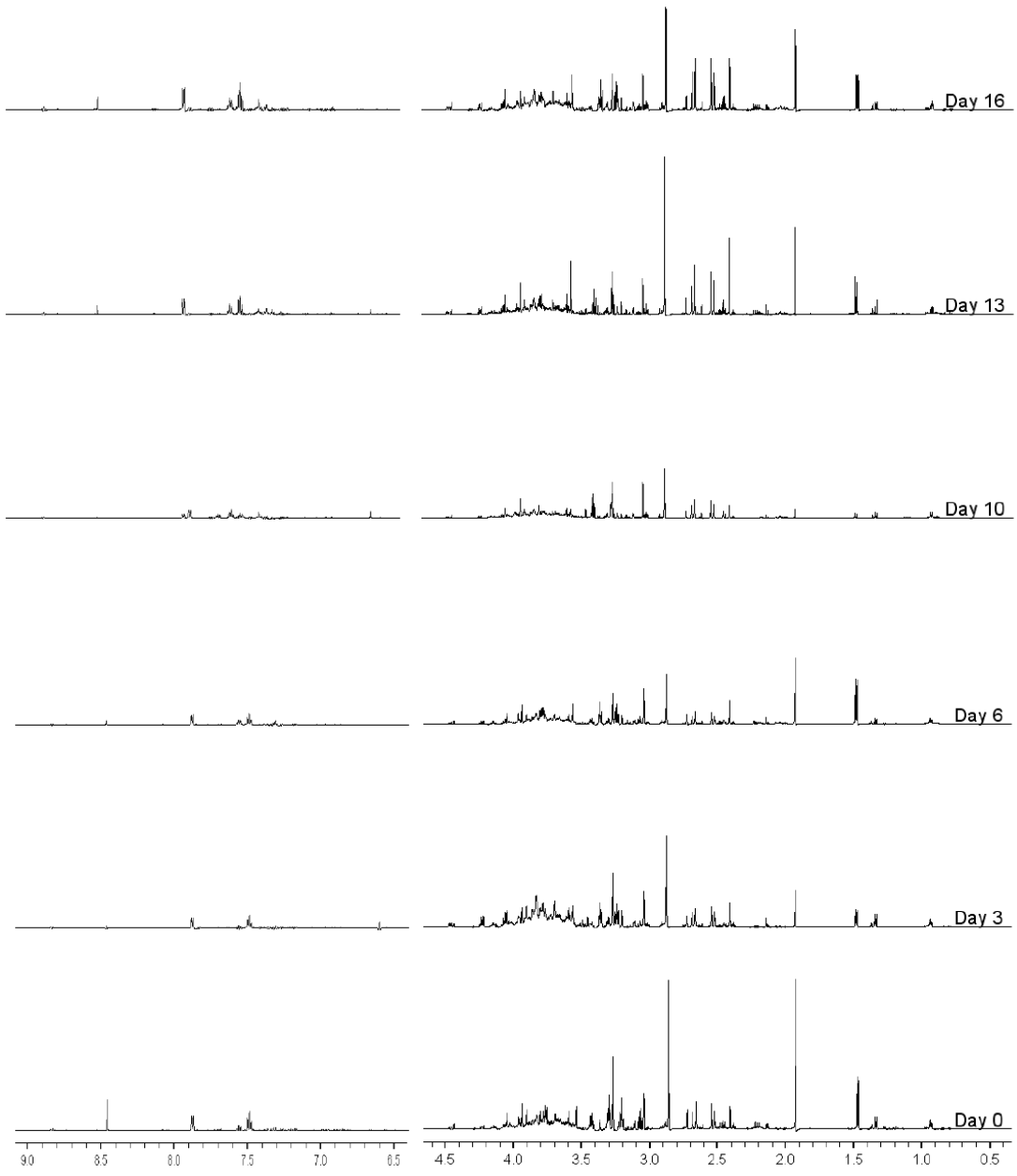

Figure 31. Representative urine NMR spectra of a mouse of high dose (2236 mg/kg/day) group in the BFAJT experiment.

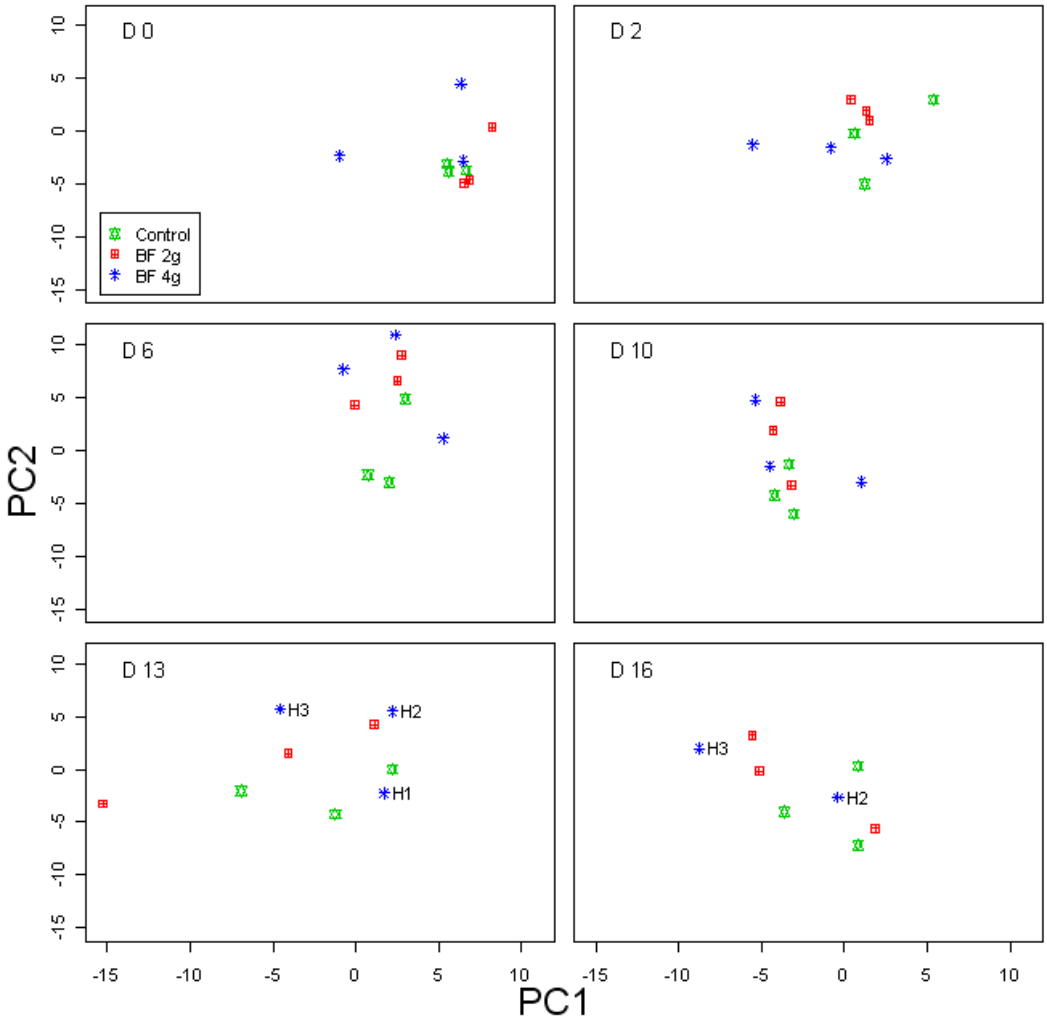

Figure 32. PCA scoring plots of mouse urine NMR spectra in the Bu-Fei-A-Jiau-Tang (BF) experiment. No group clustering from day 0 to day 16 (D16). The sum of PC1 and PC2 is 24%.

Table 2. Metabolomics studies on AA nephrotoxicity and their PCA results

Toxicants	Instrument	Equivalent AA dose, days given, route	PCA results	References
AA	^{1}H NMR	10 mg/kg/day x 5 d, i.p.	No time-dependent scoring plots between control and dose group	Zhang [1]
AM	^{1}H NMR	equivalent AA 7-10.4 mg/kg/day x 6 d, i.g.	Failure of identifying the dose group at day 6	Zhao [42]
AA	LC-MS	a single dose 50 mg/kg, i.g.	Successful group clustering at day 7; An AM group in the experiment but no PCA	Ni [41]
AA	LC-MS	10 mg/kg/day x 3 d, i.g.	Successful group clustering at day 7; No pathology available	Chan [44]

1. AM: *Aristolochia manshuriensis*
2. All experiment studied on Wistar rats and their urine samples

Table 3. Pathological grading of reanl injury in all four experiments

Animal and material (days,doses)	Toxicants weight/kg/day	Eq. dose to AA or AA-I (mg)	No. of animals	Accumulative dose (mg)	Grade of ATIN
Rat AA (5, 5)	Control	0	3	0	0
	AA 20 mg	20	3	100	0
	AA 40 mg	40	3	200	2.3
Mouse AA (12, 10)	Control	0	3	0	0
	AA 5.0 mg	5	3	50	3.7
	AA 7.5 mg	7.5	4	75	3.7 (n=3,one died)
Mouse Madouling (21, 21)	Control	0	3	0	0
	M 559 mg	0.69(AA-I)	3	14.5 (AA-I)	2
	M 1118 mg	1.38(AA-I)	3	28.9 (AA-I)	1.7
	M 2236 mg	2.75(AA-I)	3	57.8 (AA-I)	4 (n-2, one died)
Mouse BFAJT (20, 20)	Control	0	3	0	0
	BFAJT 2 g	0.25(AA-I)	3	5 (AA-I)	2
	BFAJT 4 g	0.5(AA-I)	3	10 (AA-I)	2.3

ATIN: acute tubulointerstitial nephritis

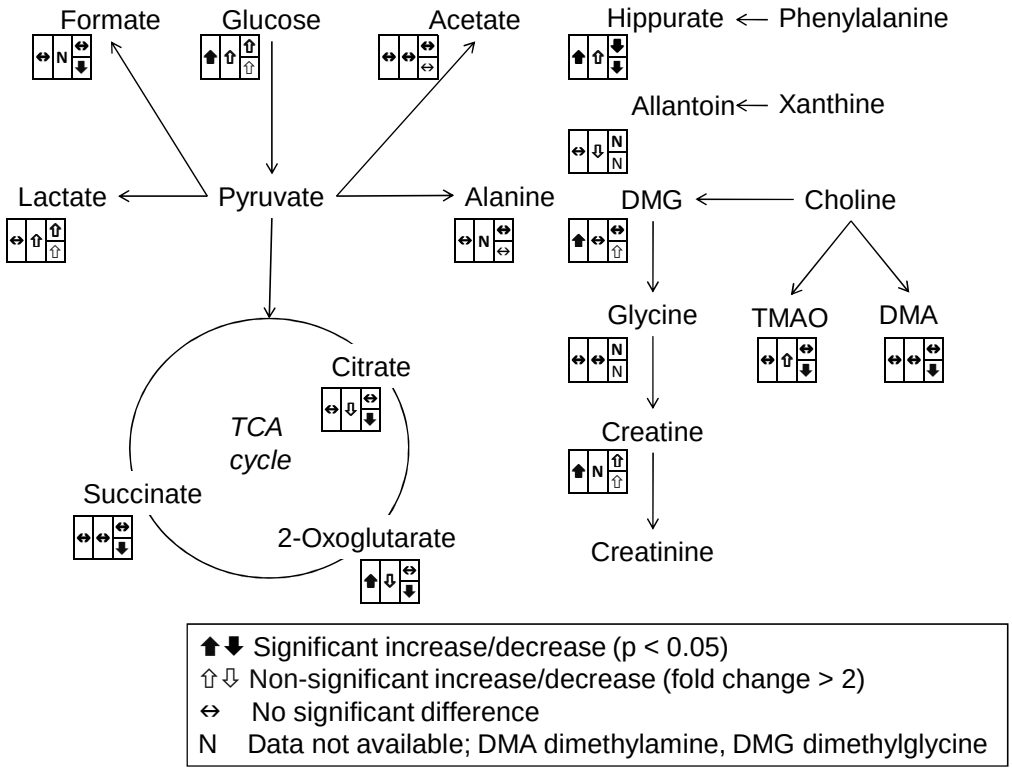

Figure 33. Metabolites in their metabolic pathways and concentration changes. Comparison of our rat AA experiment with two other experiments usign rats are shown in the left lower panels of metabolites detected in our urine NMR spectroscopy. The most left panel indicated metabolite fold change between the high dose group and the control group at the time-point of day 5. The middle panel indicated changes in an rat AA experiment reported by Zhang et al., with data collected at day 10 with 10 mg/kg/day AA in the initial 5 days [1]. The right most panel column indicated changes in an gentamicin experiment with a dose of 60 mg/kg/day for the upper panel and 120 mg/kg/day for the lower panel [2]. The chemicals of both experiments were given subcutaneously .

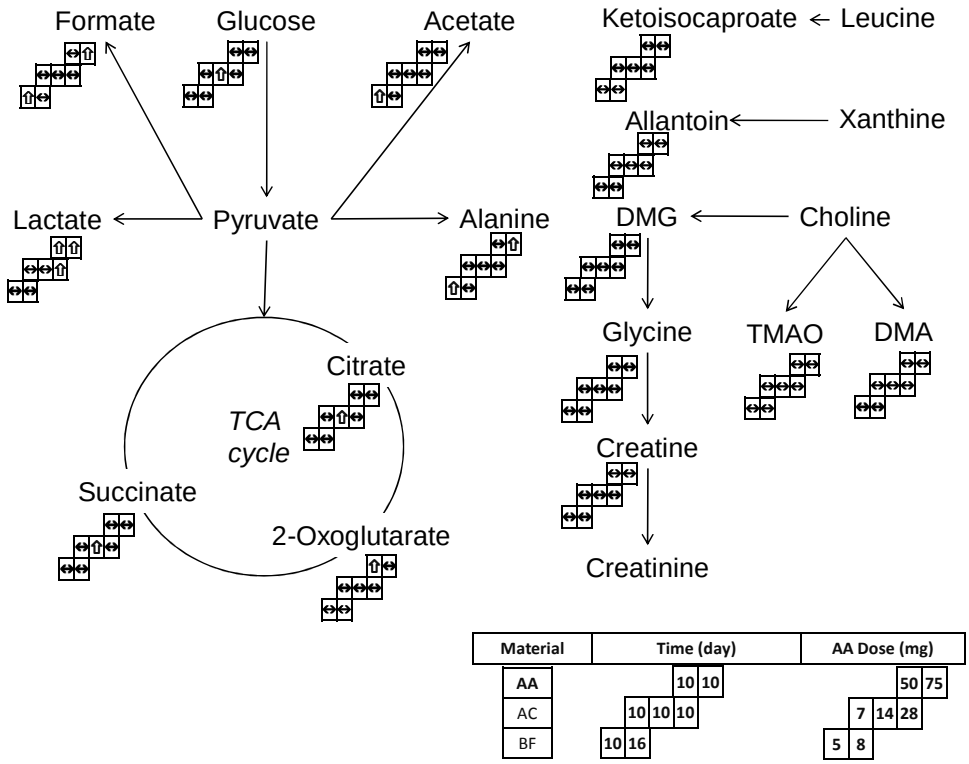

Figure 34. Metabolites detected from urine NMR spectroscopy were compared among three mouse experiments. Metabolites are shown with their metabolic pathways and concentration perturbation. Each panel recorded metabolite concentration difference with their control group. The upper row was the mouse AA experiment (AA), the left panel was the low and the right high dose group. Time point and accumulated AA dose were shown in the right lower annotation. The middle row was Madouling (AC) and low row BFAJT (BF). Concentration change symbols are referred to Figure 33.

Appendix

A. 1H NMR data preprocessing

The raw data of each 1H NMR spectrum was Fourier transformed and phased from FID signal via ACD 1D NMR manager. It is a 16384 x 2 matrix with the first column stores chemical shifts ranged from -5 to 15 ppm and the second column signal intensity at the respective chemical shifts points. The chemical shifts was approximated to fix data points with a width of 0.0001 and the signal intensity was calculated by interpolation (Figure A-1).

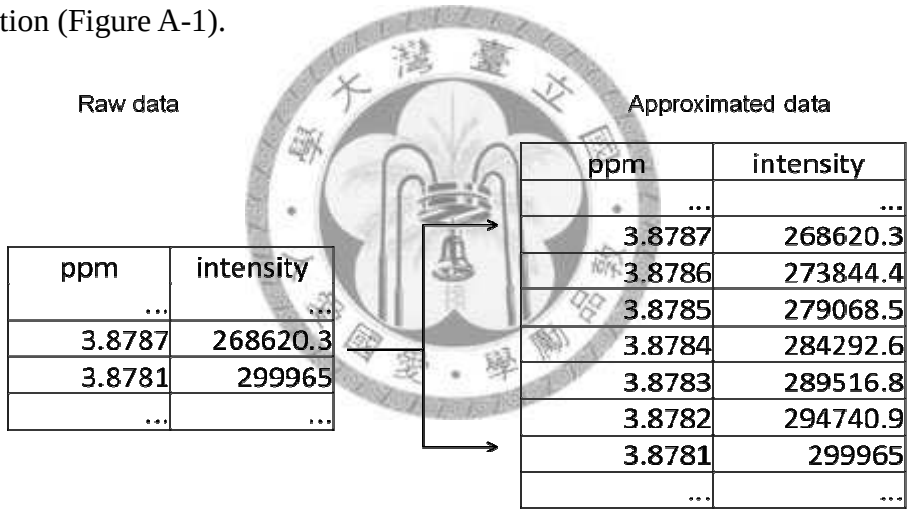

Figure A.1. The raw data contained 16384 measurement and the approximated data interpolated the measurement width to 0.0001 ppm.

After chemical shifts approximation and interpolation of signal intensities, a baseline correction was performed. A method proposed by Golotvin et. al. was applied [66]. The first step was to find a minimal noise standard deviation. The data was divided into 32 section to calculate the standard deviation of each section (σ_i), the

minimum of these standard deviation was set as to reference value σ (A.1).

$$\sigma=\min(\sigma_i),\ i=1,2,\ldots,32 \qquad \text{(A.1)}$$

The baseline points along the axis of chemical shifts were assigned by a spectral window of width N, and we took N=51. A chemical shifts point y_i was assigned as a baseline point if the difference between the minimum and maximum intensities was smaller than 2σ (A.2).

y_i is a baseline point if $(a^{max}-a^{min})<2\sigma$ (A.2)

a^{max}=max(signal intensities of chemical shifts from $y_{(i-30)}$ to $y_{(i+30)}$) (A.3)

a^{min}=min(signal intensities of chemical shifts from $y_{(i-30)}$ to $y_{(i+30)}$) (A.4)

The line along the baseline points was smoothed by a smoothing model. Here we set a range of 2M and we took M=10, and a_i' is a smoothed baseline point intensity to y_i (A.5).

$$a_i' = \sum_{k=-M}^{k=M} a_{i+k} / (2M+1),\ a_i \text{ is the signal intensity of } y_i \qquad \text{(A.5)}$$

The signal intensity of all non-baseline points was interpolated with the intensities of the two nearby smoothed intensities of baseline points. The baseline corrected data was the raw data subtraction from the baseline model, as demonstrated by an NMR spectrum (figure A.2).

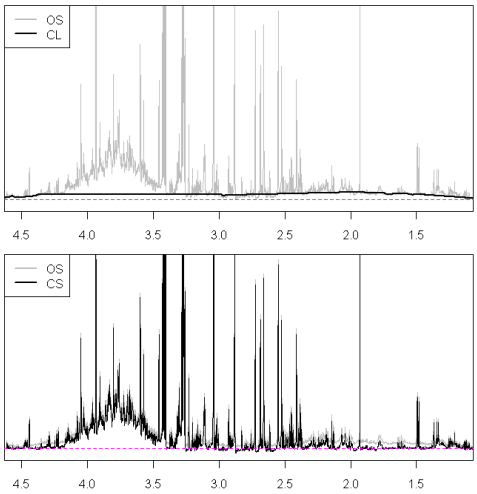

Figure A.2. A spectrum before and after baseline correction. OS: original spectrum, CL: correction baseline, CS: corrected spectrum

Next step is bucketing the baseline corrected data. The water and urea chemical shifts from 4.5 to 6.0 ppm and all negative intensities along the proton chemical shifts range was set to zero. For an approximated 0.0001 ppm chemical shifts width and baseline corrected spectrum S_j, with signal intensity a_{ji} at each chemical shifts point y_i it can be represented as a vector (A.6).

S_j=[67] , i=[50], a_{ji} is the intensity of point y_i, here y_i=0.0001i (A.6)

To bucket all spectra into bins of 0.04 ppm, we set a matrix X. X is a matrix with 250 variables labeled as 0.04, 0.08,…, 10.00 ppm. In the instance of rat AA experiment, we have 54 NMR spectra from urine samples (A.7).

$$\underset{(54\times250)}{X} = \{x_{jk}\} \quad \begin{matrix} j = 1,2,...,54 \\ k = 1,2,...,250 \end{matrix} \qquad \text{(A.7)}$$

Each row j in matrix X is intensity bins from S_j (A.8)

$$x_{jk} = \sum_{0.04(k-1)<y_i}^{y_i \le 0.04k} a_{ji} \quad , a_{ji} \text{ is the signal intensity of } y_i \qquad \text{(A.8)}$$

To scale the sum of metabolite concentration of each spectra to the same value, we applied an integral normalization (A.9). The binned elements in sample j was divided by the sum of all binned integrals of sample j and multiplied with 100 to get z_j as a scaled binned sample j spectrum.

$$z_j = \frac{x_j}{\sum_i x_{ji}} \times 100 \qquad \text{(A.9)}$$

Finally, before applying PCA to all scaled spectra, we performed a probabilistic quotient normalization (PQN) according to Dieterle F. et. al. [50]. One of the scaled binned spectrum was chosen as a reference. All other spectra were set as targets and bins of each target spectrum was divided to the respective bins of the reference spectrum. A vector of quotients was produced and its median was set to be a multiplying factor for all bins in the target spectrum. With PQN, dilution effect among urine samples can be normalized according to the majority of metabolites in a urine sample and avoid the incorporation of individual metabolite's non-dilutional pathological concentration change.

B. PCA

The scaled binned and PQN treated spectra Z were then used for PAC.

After deleting columns of all zero elements, we construct a correlation matrix.

$$\underset{(p\times p)}{R} = \tilde{Z}'\tilde{Z} \tag{B.1}$$

p is the number of columns with at least on non-zero element.

$$\underset{(j\times p)}{\tilde{Z}} = \left\{z_{ji'}\right\}, i' = i \text{ of } \sum_{i=1}^{54} z_{ji} \neq 0 \tag{B.2}$$

PCA is performed by decomposing matrix R to get a score matrix T.

$$R = T'\Lambda T \tag{B.3}$$

T is the matrix of all eigenvectors and Λ is a diagonal matrix of eigenvalues.

Now we have matrix Y with row 1 represents principal component 1 (PC1) of all samples and row 2 PC2.

$$Y = \tilde{Z}T \tag{B.4}$$

We constructed screeplot to visualize the distribution of eigenvalues. A two dimensional score plot was built with PC1 and PC2 values in matrix Y to visualize distribution of all samples.

A loading plot was built with PC1 and PC2 values in matrix T.

All procedures and plots were performed by written programs with R language and executed under R version 2.81 environment.

Bibliography

1. Zhang X, Wu H, Liao P, Li X, Ni J, Pei F: NMR-based metabonomic study on the subacute toxicity of aristolochic acid in rats. *Food Chem Toxicol* 2006, 44:1006-1014.

2. Sieber M, Hoffmann D, Adler M, Vaidya VS, Clement M, Bonventre JV, Zidek N, Rached E, Amberg A, Callanan JJ, et al: Comparative Analysis of Novel Noninvasive Renal Biomarkers and Metabonomic Changes in a Rat Model of Gentamicin Nephrotoxicity. *Toxicol Sci* 2009, 109:336-349.

3. Li X, Wang H: Aristolochic acid nephropathy: what we know and what we have to do. *Nephrology (Carlton)* 2004, 9:109-111.

4. Debelle FD, Vanherweghem J-L, Nortier JL: Aristolochic acid nephropathy: A worldwide problem. *Kidney Int* 2008, 74:158-169.

5. Feigin VL: Herbal medicine in stroke: does it have a future? *Stroke* 2007, 38:1734-1736.

6. Kessler RC, Davis RB, Foster DF, Van Rompay MI, Walters EE, Wilkey SA, Kaptchuk TJ, Eisenberg DM: Long-term trends in the use of complementary and alternative medical therapies in the United States. *Ann Intern Med* 2001, 135:262-268.

7. Molassiotis A, Potrata B, Cheng KK: A systematic review of the effectiveness of

Chinese herbal medication in symptom management and improvement of quality of life in adult cancer patients. *Complement Ther Med* 2009, 17:92-120.

8. Messina BA: Herbal supplements: Facts and myths--talking to your patients about herbal supplements. *J Perianesth Nurs* 2006, 21:268-278.

9. Vanherweghem JL, Depierreux M, Tielemans C, Abramowicz D, Dratwa M, Jadoul M, Richard C, Vandervelde D, Verbeelen D, Vanhaelen-Fastre R, et al.: Rapidly progressive interstitial renal fibrosis in young women: association with slimming regimen including Chinese herbs. *Lancet* 1993, 341:387-391.

10. Debelle FD, Nortier JL, De Prez EG, Garbar CH, Vienne AR, Salmon IJ, Deschodt-Lanckman MM, Vanherweghem JL: Aristolochic acids induce chronic renal failure with interstitial fibrosis in salt-depleted rats. *J Am Soc Nephrol* 2002, 13:431-436.

11. Lemy A, Wissing KM, Rorive S, Zlotta A, Roumeguere T, Muniz Martinez MC, Decaestecker C, Salmon I, Abramowicz D, Vanherweghem JL, Nortier J: Late onset of bladder urothelial carcinoma after kidney transplantation for end-stage aristolochic acid nephropathy: a case series with 15-year follow-up. *Am J Kidney Dis* 2008, 51:471-477.

12. Cosyns JP, Dehoux JP, Guiot Y, Goebbels RM, Robert A, Bernard AM, van Ypersele de Strihou C: Chronic aristolochic acid toxicity in rabbits: a model of

Chinese herbs nephropathy? *Kidney Int* 2001, 59:2164-2173.

13. Arlt VM, Stiborova M, Schmeiser HH: Aristolochic acid as a probable human cancer hazard in herbal remedies: a review. *Mutagenesis* 2002, 17:265-277.

14. 刘炜: 补肺阿胶汤在呼吸系统疾患中的临床运用. *黑龙江中医药* 2003:29-30.

15. 蘇喜改, 張蘭桐, 袁志芳, 田葆萍: 關木通和龍膽瀉肝丸中馬兜鈴酸 A 在大鼠體內的藥動學比較. *醫藥導報* 2005:116-118.

16. 嚴尚學, 朱成舉, 黃德武, 陳鳳芹: 龍膽瀉肝顆粒的保肝利膽作用研究. *安徽醫科大學學報* 2005:327-329.

17. Yang CS, Lin CH, Chang SH, Hsu HC: Rapidly progressive fibrosing interstitial nephritis associated with Chinese herbal drugs. *Am J Kidney Dis* 2000, 35:313-318.

18. Chang CH, Wang YM, Yang AH, Chiang SS: Rapidly progressive interstitial renal fibrosis associated with Chinese herbal medications. *Am J Nephrol* 2001, 21:441-448.

19. Balachandran P, Wei F, Lin RC, Khan IA, Pasco DS: Structure activity relationships of aristolochic acid analogues: toxicity in cultured renal epithelial cells. *Kidney Int* 2005, 67:1797-1805.

20. Shibutani S, Dong H, Suzuki N, Ueda S, Miller F, Grollman AP: Selective

toxicity of aristolochic acids I and II. *Drug Metab Dispos* 2007, 35:1217-1222.

21. Mei N, Arlt VM, Phillips DH, Heflich RH, Chen T: DNA adduct formation and mutation induction by aristolochic acid in rat kidney and liver. *Mutat Res* 2006, 602:83-91.

22. Mengs U: Acute toxicity of aristolochic acid in rodents. *Arch Toxicol* 1987, 59:328-331.

23. Mengs U, Stotzem CD: Renal toxicity of aristolochic acid in rats as an example of nephrotoxicity testing in routine toxicology. *Arch Toxicol* 1993, 67:307-311.

24. Sato N, Takahashi D, Chen SM, Tsuchiya R, Mukoyama T, Yamagata S, Ogawa M, Yoshida M, Kondo S, Satoh N, Ueda S: Acute nephrotoxicity of aristolochic acids in mice. *J Pharm Pharmacol* 2004, 56:221-229.

25. Mengs U, Lang W, Poch JA: The carcinogenic action of aristolochic acid in rats. *Archives of Toxicology* 1982, 51:107-119.

26. Pozdzik AA, Salmon IJ, Debelle FD, Decaestecker C, Van den Branden C, Verbeelen D, Deschodt-Lanckman MM, Vanherweghem JL, Nortier JL: Aristolochic acid induces proximal tubule apoptosis and epithelial to mesenchymal transformation. *Kidney Int* 2008, 73:595-607.

27. Wen YJ, Qu L, Li XM: Ischemic injury underlies the pathogenesis of aristolochic acid-induced acute kidney injury. *Transl Res* 2008, 152:38-46.

28. Star RA: Treatment of acute renal failure. *Kidney Int* 1998, 54:1817-1831.

29. Keyes R, Bagshaw SM: Early diagnosis of acute kidney injury in critically ill patients. *Expert Review of Molecular Diagnostics* 2008, 8:455-464.

30. Hauet T, Baumert H, Gibelin H, Hameury F, Goujon JM, Carretier M, Eugene M: Noninvasive monitoring of citrate, acetate, lactate, and renal medullary osmolyte excretion in urine as biomarkers of exposure to ischemic reperfusion injury. *Cryobiology* 2000, 41:280-291.

31. Han WK, Waikar SS, Johnson A, Betensky RA, Dent CL, Devarajan P, Bonventre JV: Urinary biomarkers in the early diagnosis of acute kidney injury. *Kidney Int* 2008, 73:863-869.

32. Albright RC, Jr.: Acute renal failure: a practical update. *Mayo Clin Proc* 2001, 76:67-74.

33. Shiu SH, Borevitz JO: The next generation of microarray research: applications in evolutionary and ecological genomics. *Heredity* 2008, 100:141-149.

34. Portilla D, Schnackenberg L, Beger RD: Metabolomics as an extension of proteomic analysis: study of acute kidney injury. *Semin Nephrol* 2007, 27:609-620.

35. Gates SC, Sweeley CC: Quantitative metabolic profiling based on gas chromatography. *Clin Chem* 1978, 24:1663-1673.

36. Nicholson JK, Lindon JC, Holmes E: 'Metabonomics': understanding the metabolic responses of living systems to pathophysiological stimuli via multivariate statistical analysis of biological NMR spectroscopic data. *Xenobiotica* 1999, 29:1181-1189.

37. Fiehn O: Metabolomics – the link between genotypes and phenotypes. *Plant Molecular Biology* 2002, 48:155-171.

38. Nicholson JK, Foxall PJ, Spraul M, Farrant RD, Lindon JC: 750 MHz 1H and 1H-13C NMR spectroscopy of human blood plasma. *Anal Chem* 1995, 67:793-811.

39. Mayr M: Metabolomics: Ready for the Prime Time? *Circ Cardiovasc Genet* 2008, 1:58-65.

40. Chen M, Su M, Zhao L, Jiang J, Liu P, Cheng J, Lai Y, Liu Y, Jia W: Metabonomic study of aristolochic acid-induced nephrotoxicity in rats. *J Proteome Res* 2006, 5:995-1002.

41. Ni Y, Su M, Qiu Y, Chen M, Liu Y, Zhao A, Jia W: Metabolic profiling using combined GC-MS and LC-MS provides a systems understanding of aristolochic acid-induced nephrotoxicity in rat. *FEBS Lett* 2007, 581:707-711.

42. Zhao JY, Yan XZ, Peng SQ: Metabonomics study on nephrotoxicity of Aristolochia manshuriensis. *Chinese Traditional and Herbal Drugs* 2006,

37:726-730.

43. Chan W, Cai Z: Aristolochic acid induced changes in the metabolic profile of rat urine. *J Pharm Biomed Anal* 2008, 46:757-762.

44. Chan W, Lee KC, Liu N, Wong RN, Liu H, Cai Z: Liquid chromatography/mass spectrometry for metabonomics investigation of the biochemical effects induced by aristolochic acid in rats: the use of information-dependent acquisition for biomarker identification. *Rapid Commun Mass Spectrom* 2008, 22:873-880.

45. Zhang X, Wu HF, Li XJ, Pei FK, Ni JZ: NMR Studies on the Subacute Biochemical Effects of Aristolochic Acid on Rat Serum. *Chinese Chemical Letters* 2005, 16:1507-1510.

46. 赵剑宇, 颜贤忠, 彭双清: 利用代谢组学技术研究中药关木通的肾毒性作用. *世界科学技术-中医药现代化* 2007, 9:54-59.

47. 趙劍宇, 顏賢忠, 彭雙清: 關木通腎毒性的代謝組學研究. *中草藥* 2006, 37:725-730.

48. Yue H, Chan W, Guo L, Cai Z: Determination of aristolochic acid I in rat urine and plasma by high-performance liquid chromatography with fluorescence detection. *Journal of Chromatography B* 2009, 877:995-999.

49. Huljic S, Bruske EI, Pfitzenmaier N, O'Brien E, Dietrich DR: Species-specific toxicity of aristolochic acid (AA) in vitro. *Toxicol In Vitro* 2008, 22:1213-1221.

50. Dieterle F, Ross A, Schlotterbeck G, Senn H: Probabilistic quotient normalization as robust method to account for dilution of complex biological mixtures. Application in 1H NMR metabonomics. *Anal Chem* 2006, 78:4281-4290.

51. Van QN, Issaq HJ, Jiang Q, Li Q, Muschik GM, Waybright TJ, Lou H, Dean M, Uitto J, Veenstra TD: Comparison of 1D and 2D NMR spectroscopy for metabolic profiling. *J Proteome Res* 2008, 7:630-639.

52. Kim S, Wang Z, Hiremath B: A Bayesian approach for the alignment of high-resolution NMR spectra. *Annals of Operations Research* 2008, Mar.

53. Craig A, Cloarec O, Holmes E, Nicholson JK, Lindon JC: Scaling and normalization effects in NMR spectroscopic metabonomic data sets. *Anal Chem* 2006, 78:2262-2267.

54. Park JC, Hong YS, Kim YJ, Yang JY, Kim EY, Kwack SJ, Ryu do H, Hwang GS, Lee BM: A metabonomic study on the biochemical effects of doxorubicin in rats using (1)H-NMR spectroscopy. *J Toxicol Environ Health A* 2009, 72:374-384.

55. Cloarec O, Dumas ME, Craig A, Barton RH, Trygg J, Hudson J, Blancher C, Gauguier D, Lindon JC, Holmes E, Nicholson J: Statistical total correlation spectroscopy: an exploratory approach for latent biomarker identification from metabolic 1H NMR data sets. *Anal Chem* 2005, 77:1282-1289.

56. Holmes E, Bonner FW, Nicholson JK: Comparative studies on the nephrotoxicity of 2-bromoethanamine hydrobromide in the Fischer 344 rat and the multimammate desert mouse (Mastomys natalensis). *Arch Toxicol* 1995, 70:89-95.

57. Shackelford C, Long G, Wolf J, Okerberg C, Herbert R: Qualitative and quantitative analysis of nonneoplastic lesions in toxicology studies. *Toxicol Pathol* 2002, 30:93-96.

58. Wishart DS, Tzur D, Knox C, Eisner R, Guo AC, Young N, Cheng D, Jewell K, Arndt D, Sawhney S, et al: HMDB: the Human Metabolome Database. *Nucleic Acids Res* 2007, 35:D521-526.

59. Bollard ME, Keun HC, Beckonert O, Ebbels TM, Antti H, Nicholls AW, Shockcor JP, Cantor GH, Stevens G, Lindon JC, et al: Comparative metabonomics of differential hydrazine toxicity in the rat and mouse. *Toxicol Appl Pharmacol* 2005, 204:135-151.

60. Martin FP, Dumas ME, Wang Y, Legido-Quigley C, Yap IK, Tang H, Zirah S, Murphy GM, Cloarec O, Lindon JC, et al: A top-down systems biology view of microbiome-mammalian metabolic interactions in a mouse model. *Mol Syst Biol* 2007, 3:112.

61. Drickamer L: Rates of urine excretion by house mouse (Mus domesticus):

Differences by age, sex, social status, and reproductive condition. *Journal of Chemical Ecology* 1995, 21:1481-1493.

62. Um SY, Chung MW, Kim KB, Kim SH, Oh JS, Oh HY, Lee HJ, Choi KH: Pattern recognition analysis for the prediction of adverse effects by nonsteroidal anti-inflammatory drugs using 1H NMR-based metabolomics in rats. *Anal Chem* 2009, 81:4734-4741.

63. Saric J, Li JV, Wang Y, Keiser J, Bundy JG, Holmes E, Utzinger J: Metabolic Profiling of an Echinostoma caproni Infection in the Mouse for Biomarker Discovery. *PLoS Negl Trop Dis* 2008, 2:e254.

64. Wang Y, Holmes E, Nicholson JK, Cloarec O, Chollet J, Tanner M, Singer BH, Utzinger J: Metabonomic investigations in mice infected with Schistosoma mansoni: An approach for biomarker identification. *Proceedings of the National Academy of Sciences of the United States of America* 2004, 101:12676-12681.

65. Espandiari P, Zhang J, Rosenzweig BA, Vaidya VS, Sun J, Schnackenberg L, Herman EH, Knapton A, Bonventre JV, Beger RD, et al: The utility of a rodent model in detecting pediatric drug-induced nephrotoxicity. *Toxicol Sci* 2007, 99:637-648.

66. Golotvin S, Williams A: Improved baseline recognition and modeling of FT NMR spectra. *J Magn Reson* 2000, 146:122-125.

67. Suzuki H, Sasaki R, Ogata Y, Nakamura Y, Sakurai N, Kitajima M, Takayama H, Kanaya S, Aoki K, Shibata D, Saito K: Metabolic profiling of flavonoids in Lotus japonicus using liquid chromatography Fourier transform ion cyclotron resonance mass spectrometry. *Phytochemistry* 2008, 69:99-111.